Unnaturalness in the evolution process of the SARS-CoV-2 variants and the possibility of deliberate natural selection

Authors: Atsushi Tanaka[1,2,*], Takayuki Miyazawa[2,3,*]

[1)]Division of Research Animal Laboratory and Translational Medicine, Research and Development Center Osaka Medical and Pharmaceutical University, Takatsuki, Osaka 569-8686, Japan

[2)]Laboratory of Virus-Host Coevolution, Institute for Life and Medical Sciences, Kyoto University, Sakyo-ku, Kyoto 606-8507, Japan

[3)] Resilience Research Unit, Kyoto University, Katsura, Nishikyo-ku, Kyoto 615-8540, Japan

***Corresponding authors:**

Dr. Atsushi Tanaka, Division of Research Animal Laboratory and Translational Medicine, Research and Development Center Osaka Medical and Pharmaceutical University, Takatsuki, Osaka 569-8686, Japan

E-mail: atsushi.tanaka@ompu.ac.jp

Dr. Takayuki Miyazawa, Laboratory of Virus-Host Coevolution, Institute for Life and Medical Sciences, Kyoto University, 53 Shogoin-Kawaharacho, Sakyo-ku, Kyoto 606-8507, Japan.

E-mail: takavet@infront.kyoto-u.ac.jp

Phone: +81-(0)75-751-4814

Running head: Unnatural evolution of the SARS-CoV-2 variants

Abstract

Over the past three years, severe acute respiratory syndrome coronavirus 2 (SARS-CoV-2) has repeatedly experienced pandemics, generating various mutated variants ranging from Alpha to Omicron. In this study, we aimed to clarify the evolutionary processes leading to the formation of SARS-CoV-2 Omicron variants, focusing on Omicron variants with many amino acid mutations in the spike protein among SARS-CoV-2 isolates. To determine the order in which the mutations leading to the formation of the SARS-CoV-2 Omicron variants, we compared the sequences of 129 Omicron BA.1-related isolates, 141 BA.1.1-related isolates, and 122 BA.2-related isolates, and tried to dissolve the evolutionary processes of the SARS-CoV-2 Omicron variants, including the order of mutations leading to the formation of the SARS-CoV-2 Omicron variants and the occurrence of homologous recombination. As a result, we concluded that the formations of a part of Omicron isolates BA.1, BA.1.1, and BA.2 were not the products of genome evolution as is commonly observed in nature, such as the accumulation of mutations and homologous recombinations. Furthermore, the study of 35 recombinant isolates of Omicron variants BA.1 and BA.2, confirmed that Omicron variants were already present in 2020. The analysis we have shown here is that the Omicron variants are formed by an entirely new mechanism that cannot be explained by previous biology, and knowing the way how the SARS-CoV-2 variants were formed prompts a reconsideration of the SARS-CoV-2 pandemic.

Introduction

COVID-19, the coronavirus disease 2019, caused by severe acute respiratory syndrome coronavirus 2 (SARS-CoV-2), was first reported in December 2019 in Wuhan, China (1). This emerging infectious disease has been unprecedentedly fast, diffusing worldwide, leading the World Health Organization (WHO) to declare a global pandemic of COVID-19 on March 11, 2020 (https://www.who.int/). SARS-CoV-2, belonging to betacoronavirus subgroup B, has a single-stranded positive-sense RNA genome that codes for ten genes, ultimately producing 26 proteins according to an annotation of NCBI Reference Sequence: NC_045512.2. Its genome size varies from 29.8 kb to 29.9 kb. It consists of four structural proteins: spike (S), envelope (E), membrane (M), and nucleocapsid (N) proteins (2, 3). In the structural proteins, the S protein as the surface glycoprotein is the largest protein, approximately 180 kDa, consisting of two subunits, S1 and S2. It mediates membrane fusion and ultimately facilitates virus entry. The receptor binding domain (RBD) (amino acid residues 319−541) of the S1 subunit interacts with the angiotensin-converting enzyme 2 (ACE2), binding to its peptidase domain (4, 5).

Over the past three years (2019-2022), SARS-CoV-2 was re-accelerated by new variants that emerged over several months in various geographical regions and then transferred over the world, then induced the pandemic repeatedly.

In the early stage of the first pandemic, the most impactful mutation of SARS-CoV-2 was a non-synonymous mutation D614G in the S protein. This mutation, which was not present in the ancestral lineage that caused the Wuhan outbreak, became quickly dominant worldwide (6). Soon later, the variant of concern,

B.1.1.7 : 20I (Alpha, V1), the lineage B.1.1.7 (clade 501.YV1) or Alpha, characterized by 17 unique mutations containing ten amino acids differences in the S protein, was first detected in southeastern England in late September 2020 (7) and expanded rapidly across the United Kingdom to become predominant during early 2021, spreading to most European countries with similar success. By November 2021, local transmission of this lineage had been reported in 175 countries (8). Shortly after that, the emergence of variant strains of SARS-CoV-2 Alpha, variants B.1.351 : 20H (Beta, V2) was identified in October 2020, which was first detected in the Eastern Cape province of South Africa from specimens collected in early August. This Beta variant was spread within South Africa and appeared to have displaced the other SARS-CoV-2 lineages circulating there (9). Then the variant P.1: 20J (Gamma, V3) was identified in Brazil in December 2020 that appeared to have evolved in Brazil. Health officials in Japan first reported it publicly on January 10, 2021, after finding the Gamma variant in four Brazilian travelers at Haneda Airport in Tokyo, Japan (10).

At about the same time, the Delta variant (Pango lineage designation B.1.617.2), which was first detected in India in February 2021, and the Mu variant, also known as lineage B.1.621 first detected in Colombia in January 2021were reported (11, 12).

Almost one year later, these emergences of variants of concern, Omicron (phylogenetic assignment of named global outbreak (Pango) lineage designation B.1.1.529; BA.1, Nextstrain clade 21K) is a variant of SARS-CoV-2 first reported to the WHO by the Network for Genomics Surveillance in South Africa on November 24, 2021 (13, 14) that has more than 50 amino acids changes when compared with first reported strain Wuhan-Hu-H1 (NCBI Reference Sequence: NC_045512.2.), and 39 amino acids difference of them were

observed in the S protein. This variant was first detected in Botswana and has become the predominant circulating variant worldwide (15).

In the United States, the San Francisco Department of Public Health has confirmed a case of COVID-19 among individuals in California was caused by the Omicron variant BA.1, which transferred from a traveler who returned from South Africa on November 22, 2021 (https://www.cdc.gov/media/releases/2021/s1201-Omicron-variant.html). Then, the first Omicron sub-lineage BA.1, expanded rapidly and replaced the Delta variant (16).

Soon after (less than two weeks after), the first identification of the Omicron variant BA.1, the new Omicron variant, BA.2 lineage, which has 31 amino acids changes in the S protein when compared with the Wuhan-Hu-H1 in Denmark on December 5, 2021 (17). On February 22, 2022, WHO mentioned on the Omicron sublineage BA.2 (https://www.who.int/news/item/22-02-2022-statement-on-Omicron-sublineage-ba.2) that the Omicron variant of concern was currently the dominant variant circulating globally, replacing the Delta variant (Pango lineage designation B.1.617.2) (https://www.who.int/docs/default-source/coronaviruse/2022-01-07-global-technical-brief-and-priority-action-on-Omicron---corr2.pdf?sfvrsn=918b09d_20), accounting for nearly all sequences reported to GISAID. Then as of March 16, 2023, WHO stated that the Omicron variants account for over 98% of the publicly available viral sequences since February 2022 (https://www.who.int/news/item/16-03-2023-statement-on-the-update-of-who-s-working-definitions-and-tracking-system-for-SARS-CoV-2-variants-of-concern-and-variants-of-interest).

93 The Omicron variants BA.1 and BA.2 are suggested to have expanded and diverged around October to
94 December 2021, respectively. These mutants are estimated to diverge from the common ancestor around
95 February to March 2021 (18). Since the Omicron variants BA.1 and BA.2 share a common 14 amino acids
96 mutation in the S protein, the common ancestor of Omicron variants BA.1 and BA.2 may have already acquired
97 the 14 amino acid mutation in the S protein region around February to March 2021; however, no common
98 ancestral strain has been found in the international databases, and the strains may have acquired their mutations
99 through different pathways.

100 In this study, we tried to dissolve the evolution process of the Omicron variant, which has twice more
101 amino acid mutations in the S protein than other variants, by examining the rank order of introduction of amino
102 acid mutations in the S protein.

103

104 **Results**

105 Each variant is thought to have arisen through an independent evolutionary pathway from isolates with
106 the D614G mutation in the S protein. In the genetic variation in the S protein in these variants, most of the
107 mutations were non-synonymous (Fig. 1). There were no synonymous mutations in the Alpha, Beta, Gamma,
108 Delta, or Mu variants, but only one each in the Lambda and Omicron variants. Among these variants, the
109 Omicron variant (BA.1 lineage), which shows the greatest accumulation of mutations in the S protein, is
110 primarily non-synonymous in the S protein and has only one synonymous mutation at c25000u. The

111 synonymous/non-synonymous ratio is abnormal, given how human coronaviruses have mutated (See
112 Supplemental Figure 1).

113 At first, we presumed the existence of the isolate of SARS-CoV-2, whose amino acid sequence of S
114 protein contains the Omicron-BA.1-type mutation subsets, but one mutation position was not mutated and
115 constituted with the original Wuhan-type amino acid sequence. We designated these isolates as BA.1-01. Each
116 amino acid sequence of the S protein region was named the BA.1-0.1_S: amino acids of Omicron-BA.1 type
117 (Oaa) and Wuhan type (Waa) and its position number (XXX) (Ex., BA.1-0.1_S:OaaXXXWaa), as described
118 in the Methods section. And then, the putative isolates bearing the BA.1-0.1_S:OaaXXXWaa, were searched
119 using the BLAST program by their amino acid sequences. In this search, we obtained the isolates whose
120 identities is the 100% matches with the query amino acid sequence except for the SARS-CoV-
121 2_human_USA_NY-PV55373_2022(GenBank: ON246090.1) whose percent identities was 99.92%.

122 Surprisingly, we found that the Omicron BA.1-0.1 isolates were detected at all mutation sites except
123 N501Y (Fig. 2A). In the BA.1 lineage of the Omicron variant, there are Omicron isolates (BA.1.1) with the
124 R346K mutation seen in the Mu(m) variant (termed B.1.621), *i.e.*, BA.1_S can be defined as BA.1.1_S:K346R.
125 We also performed a BLAST search for isolates with amino acid sequences of BA.1-0.1.1_S:OaaXXXWaa, as
126 described in the Methods section. As a result, Omicron BA.1.1-subset-0.1 isolates were detected at all mutation
127 sites except S373P (Fig. 2B). Similar to the BA.1 lineage of the Omicron variant, in the BA.2 lineage of the
128 Omicron variant, isolates of BA.2-0.1 were found at all mutant sites except T478K and P681H in the S protein
129 (Supplemental Figure 2). The presence of these isolates refutes the establishment of Omicron strains through a

continuous evolutionary process by accumulating mutations. So, we could not determine which mutation occurred first or last in forming the Omicron variants. As shown in Fig. 2B, over half of the BA.1.1-0.1 isolates have the synonymous mutation c21595u detected in the S protein. However, this does not explain in what order the c21595u mutation arose. Curiously, in the BA.1 strain isolates, this c21595u mutation was only detected in SARS-CoV-2_human_USA_ID-CDC-LC0481844_2022 (GenBank: OM409228.1) and SARS-CoV-2_human_USA_MI-CDC- ASC210597972_2022 (GenBank: OM396816.1). These isolates commonly lack the G339D mutation. This synonymous mutation is in a mutation-prone hotspot location. Still, if the same mutation occurred independently in different isolates, it is highly unnatural that the proportion of c21595u occurrences is significantly biased in the Omicron variants BA.1.1-0.1.

It has been reported that two different variants were infected in a single cell while establishing various SARS-CoV-2 variants, causing homologous recombination in the viral RNA synthesis process, resulting in multiple variants. Assuming that homologous recombination caused the isolates shown in Fig. 2, some of the breakpoints at which strand changes occur by homologous recombination are too short (1nt, 2nt, 3nt, etc.) (Fig. 3 and Supplemental Figure 3). Therefore, it is unreasonable to use homologous recombination as the basis for establishing these isolates. Also, most of these isolates were found in the USA between 2021 and 2022; however, considering that the major prevalent variant in the USA in August 2021 was the Delta variant, it is most unlikely that it did not cause mutations such as T478K and D614G, which are already prevalent. It is inconceivable that the oldest variants (such as T478K and D614G), which are no longer prevalent, were present enough to cause superinfection and to have been involved in homologous recombination. Also, most of these isolates were

isolated in the USA between 2021 and 2022. Still, given that the isolates primarily prevalent in the USA in August 2021 were Delta variants, it is unlikely that an older type of variant without the T478K or D614G mutation was present to cause superinfection and involved in homologous recombination. This assumption is supported by the fact that all of these BA.1-0.1 isolates and BA.1.1-0.1 isolates retained the sequence of the BA.1 lineage in all regions except the S protein (Fig. 4). In addition, the fact that all of these BA.1-0.1 and BA.1.1-0.1 strains retain the sequence of Omicron strain BA.1 except for the S protein also makes it unreasonable to assume that these isolates arose by homologous recombination with an older type of mutant without the T478K or D614G mutations (Fig. 4).

Furthermore, some of the BA.1 isolates and BA.1-0.1 isolates have mutation subsets (synonymous: u10135c, ORF3: L106F, N: D343G) upstream and downstream of the S gene and the u10135c and L106F (ORF3) mutations correspond perfectly. Therefore, it is considered homologous recombination between the BA.1 variant and the variants without these mutations did not occur during the mutants' formation processes (Fig. 4). The synonymous mutation c2470u occurred in BA.1.1 compared to BA.1.1, and this c2470u mutation was retained by most but a few isolates of the BA.1.1-0.1 isolates (SARS-CoV-2_human_USA_IL-CDC-ASC210695497_2022：GenBank: OM770362.1; SARS-CoV-2_human_USA_NY-CDC-LC0450936_2021: GenBank: OM228453.1）. The synonymous mutation c2470u has also only been observed in a minimal number of BA.1-0.1 isolates（SARS-CoV-2_human_USA_OR-CDC-LC0470830_2022: GenBank: OM367679.1; SARS-CoV-2_human_USA_ID-CDC-LC0481844_2022: GenBank: OM409228.1; SARS-CoV-2_human_USA_MI-CDC-ASC210597972_2022: GenBank:OM396816.1; SARS-CoV-

2_human_USA_WI-CDC-LC0494047_2022: GenBank: OM500517.1). These results suggest that the establishment of BA.1-0.1 isolates and BA.1.1-0.1 isolates occur independently. On the other hand, if reversion mutations caused each of these isolates with one amino acid to the Wuhan-type, these isolates could be detected by examining an astronomical number of isolates. However, these virus strains were detected in the number of sequenced whole genome (a limited number), rather than in the astronomical numbers examined. The fact that most of these mutations occurred without synonymous mutations (Fig. 2) suggests that none of these mutations arose as a result of trial-and-error random mutations in nature. Few synonymous mutations are detected in some BA.1-0.1, BA.1.1-0.1, and BA.2-0.1 isolates (Fig. 2 and Supplemental Figure 2), as seen in other viruses (Supplemental Figure 1). The c25000u is the only synonymous mutation that did not occur until BA.1, BA.1.1, BA.2, BA.1-0.1 BA.1.1-0.1 and BA.2-0.1 isolates were formed and was not observed in previous variants such as alpha, beta, gamma, delta, etc. Nevertheless, it is very puzzling to find the occurrence of mutants with synonymous mutations such as c22120u, c24034u, c23635u, c24448u, c21811u, a23884g, c22987u, c23609a, c23413u, c23896u, c22879u, u24097a, c23893u, c24442u, u24847c, c24382u, c22264u, c22879u, c22480u, u21976c, c22480u, g24577a and u23101c in the BA.1.1, BA.1-0.1 and BA.1.1-0.1 isolates (Fig. 2 Synonymous Others), and a22948g, c23635u, c21859u, c22945u, c23701u, c22987u, a24433g, c23347u, u24640c, a24619g, c24865u, a23989g, u23047c, u24346c, c21811u, c21952u, a22753u, c23635u, c24023u, c24382u and c22572u in the BA.2-0.1 isolates (Supplemental Figure 2 Synonymous Others) after the formation of mutants with these subsets.

If two different viral variants infect a single cell simultaneously in the process of establishing various SARS-CoV-2 variants, and if homologous recombination occurs during viral RNA synthesis between the Omicron variant BA.1 lineage and the BA.2 lineage, it is expected that there are variants caused by homologous recombination between the BA.1 and BA.2 lineages.

Therefore, we also performed BLAST searches for isolates with mutant amino acid subsets of both the Omicron variants' BA.1 and BA.2 strains. We detected recombinant isolates of Omicron BA.1 and BA.2 lineages. Surprisingly, the recombinant of Omicron BA.1 and BA.2 lineages, SARS-CoV-2/human/PRI/PR-PR-UPRRP-582/2020 (GenBank: ON928946.1), was already present in Puerto Rico in 2020. Omicron (B.1.1.529) is a variant of SARS-CoV-2 first reported to the WHO by the Network for Genomics Surveillance in South Africa on November 24, 2021 (13, 14). It was first detected in Botswana and has spread to become the predominant variant in circulation worldwide (15). Following the appearance of the original B.1.1.529 variant, several subvariants of Omicron have emerged, including BA.1, BA.2, BA.3, BA.4, and BA.5 (19). Since October 2022, two subvariants of BA.5 called BQ.1 and BQ.1.1 have emerged.

The question then arose about why a recombinant strain, SARS-CoV-2/human/PRI/PR-UPRRP-582/2020 (GenBank: ON928946.1), already existed in 2020. We searched for SARS-CoV-2 isolates prevalent in Puerto Rico using the keywords "PRI", "PR-UPRRP", and "2020". Consequently, we found 29 Omicron-associated sequences in the 127 hits obtained (Fig. 5B). These results suggest that the SARS-CoV-2 lineages bearing the amino acid sequences of the S protein are identical to that of Omicron BA.1 and Omicron BA.2 lineages were already prevalent in Puerto Rico in 2020, with 15 isolates having the complete Omicron BA.1+

R346K_mut-subset (BA1.1) , 14 isolates had a synonymous substitution of c21595u. Four isolates had an amino acid sequence of the S protein perfectly matched that of Omicron BA2 (BA.2_S), and eight were Omicron BA.2-0.1 (BA.2-S:K440N).

Discussion

Several hypotheses have been proposed that the original SARS-CoV-2 virus resulted from an accidental laboratory spill. With recent developments in biotechnology, many viruses, including coronaviruses, have been artificially synthesized and used in various experiments (20-22). The artificial generation of mutant viruses in the laboratory and the study of viral phenotypes by introducing mutations is called "reverse genetics" and is a common technique in virology. It has been claimed that SARS-CoV-2 is artificially generated because of the unnatural presence of a codon (CGG) encoding a contiguous arginine at the furin cleavage site of SARS-CoV-2. This claim is refuted based on the following facts; 1) there is no logical reason for a genetically engineered virus to utilize such a suboptimal furin cleavage site. 2) The only previous study on artificial insertion of furin cleavage sites at the S1/S2 boundary of the S protein of SARS-CoV-1 using the pseudotype virus experimental system utilized the optimal "RRSRR" sequence, which is different from the furin cleavage site's sequence present in SARS-CoV-2. 3) There is also no evidence of previous studies at the Wuhan Institute of Virology that artificially inserted a complete furin cleavage site in coronaviruses. 4) Unnatural CGG codons adjacent to the arginine at the furin cleavage site are rare in coronaviruses but are observed at a particular frequency in SARS-CoV-1, SARS-CoV-2, and other human coronaviruses. However, these are only declarations and are

illogical. No one explained why a naturally occurring virus would utilize a suboptimal furin cleavage site. It has not been mentioned about technically possible to insert this furin cleavage site or a CGG codon artificially. Inserting a polybasic furin cleavage site on the S protein makes it impossible to conclude whether SARS-CoV-2 is a naturally occurring or artificial virus by discussing whether it is natural or artificial.

Despite the accumulation of many mutations in the S protein of Omicron mutants, most of the mutations are non-synonymous, with only one synonymous mutation of c25000u, which is highly unnatural, leading to the hypothesis that the Omicron mutants are artificially synthesized. The following results presented in this study may support the hypothesis that the Omicron variants may have been artificially synthesized rather than naturally occurring: 1) the presence of Omicron variant-associated isolates with one mutation site being Wuhan-type; 2) the almost complete absence of synonymous mutations in the S protein in these isolates; 3) the Omicron variant, which should have been first reported to WHO from South Africa on November 24, 2021, was already endemic in Puerto Rico in 2020, and that there were isolates that were recombinants between Omicron strains BA1 and BA2. In addition, the Omicron mutant-related isolates (BA.1-0.1, BA.1.1-0.1, and BA.2-0.1 isolates) with a Wuhan-type mutation at one of the mutation sites were established. Some had synonymous mutations after establishing the Omicron mutant-related isolates (Fig. 2 and Supplemental Figure 2 Synonymous Others). It is reasonable to assume that viruses with the reversion amino acid mutations caused by non-synonymous mutations in the S protein were artificially synthesized and then acquired further synonymous mutations in the natural environment.

Assuming that artificially synthesized mutants with only non-synonymous mutations are spread globally, this would explain how mutants with non-synonymous mutations without previous synonymous mutations develop synonymous mutations under natural circumstances. Considering the current epidemic situation of SARS-CoV-2, it is unlikely that these viruses arose spontaneously. In explaining the formation of the SARS-CoV-2 isolate, as shown here, the SARS-CoV-2 isolates are formed by a completely new mechanism that cannot be explained by previous biology.

One idea, the hypothesis that these viruses were artificially generated, is more reasonable than proposing a novel mutation acquisition mechanism. However, is there any reason to artificially create these mutants, which are unlikely to have occurred naturally, given the current SARS-CoV-2 epidemic?

It has been known that the pathogenicity, host specificity, cell tropism, and immunogenicity of numerous viruses can be altered by mutation of a single (or several) amino acid(s) of a viral protein on the viral envelope (envelope protein, HA protein, spike protein, etc.). A single-amino-acid substitution in the HA protein of the 2009 pandemic A (H1N1) influenza viruses changes their replication and pathogenicity (23). In the Chikungunya virus, single amino acid changes in the E2 glycoprotein influence glycosaminoglycan utilization for target cell binding (24) , and single amino acid change in the E1 glycoprotein affects mosquito vector specificity and epidemic potential (25). In previous coronaviruses such as MERS-CoV and SARS-CoV-1, point mutations have been demonstrated to confer resistance to neutralizing antibodies (26-28).

Suppose the SARS-CoV-2 Omicron variant and its one amino acid reversion mutants were artificially and systematically generated. In that case, we should suspect that the other variants (Alpha to Delta) may also

261 be artificially generated viruses. Indeed, the lack of findings to date that many of the various mutations seen,
262 especially in the early variants, are indeed associated with increased viral infection (29) supports the hypothesis
263 that each variant was artificially synthesized to identify the amino acids of the S protein responsible for
264 infectivity and pathogenicity. The possibility that the set of mutants was artificially generated to identify amino
265 acids of the S protein involved in the infectivity and virulence is supported.

266 Reverse genetics experiments are an essential part of virus research, and it is inimical to virus research to
267 consider that artificially synthesized viruses were deliberately spread throughout the world. However, now that
268 reverse genetics has become common in virus research, we believe it is not scientific to discuss the mutation
269 process of SARS-CoV-2 without excluding the possibility of artificially synthesized viruses.

270 Finally, we would like to add that while artificially synthesized viruses may have spread, we are not
271 criticizing reverse genetics technology, as reverse genetics technology has made tremendous advances in
272 virology. In addition, our analysis uses databases with a limited number of viral sequences, and we cannot deny
273 the possibility that unreliable data may have been registered due to technical problems in sequencing or some
274 malicious intent. Furthermore, we do not conclude that these viruses were artificially synthesized and distributed
275 based on malicious intent. This paper aims to point out that SARS-CoV-2 has undergone unthinkable mutations
276 under conventional coronavirus mutation mechanisms, and we hope that the possibility of artificial theory
277 should be included in the discussion seriously as to the formation of SARS-CoV-2 variants.

Nonetheless, the analysis we have shown here concludes that the Omicron variants are formed by a completely new mechanism that cannot be explained by previous biology. The way how the SARS-CoV-2 mutations occurred should prompt a reconsideration of the SARS-CoV-2 pandemic.

Methods

Data acquisition

SARS-CoV-2 RNA genome and genes and proteins according to an annotation of the SARS-CoV-2 Wuhan-Hu-H1 (COVID-19/Wuhan-Hu-1CHN/2019/First Isolate) NCBI Reference Sequence: NC_045512.2 were used as a reference strain for the definition of mutations and provided base of the numbering of nucleotide and amino acids number of each protein. Genome data of SARS-CoV-2 isolates which showed in this article were obtained by coping from NCBI Nucleotide database (https://www.ncbi.nlm.nih.gov/) on 25/11/2022 to 17/03/2023.

Query of representative SARS-CoV-2 variant genome

Amino acids sequences of spike protein of SARS-CoV-2 variants（Alpha:B.1.1.7, Beta:B.1.351, Gamma:P1, Delta:B.1.617.2.63, Lambda:C.37, Mu:B.1.621, Omicron:BA.1, BA.1.1 and BA.2）were obtained from internet site, Stanford Coronavirus Antiviral & Resistance Database (https://covdb.stanford.edu/) or Covariant (https://covariants.org/) and used as a query sequence for NCBI protein BLAST search (blastp: protein-protein BLAST, https://blast.ncbi.nlm.nih.gov/Blast.cgi?PROGRAM=blastp&PAGE_TYPE=BlastSearch&LINK_LOC=blasthome). Then the whole genome sequence of each variant isolates bearing the query spike sequence were derived from the BLAST search resultant which identified with query amino acids sequence with 100%. And then the nucleotide sequences of detected SARS-CoV-2 genome were as follows, GenBank Accession No.: GenBank: MW423686.2; MW430966.1; MW430967.1; MW422256.1; MW598419.1;

MW667552.1; MW667553.1; MW721502.1; MW721504.1; MW520923.1; MW642248.1; MW642249.1; MW642250.1; MZ182066.1; MZ155303.1; MZ155230.1; MZ170364.1; MZ179869.1; MW666666.1; MW696612.1; MW699217.1; MW644498.1; MZ727706.1; MZ620161.1; MZ637380.1; MZ637401.1; MZ780550.1; OL672836.1; OL677199.1; OP769083.1; OL764360.1; OL815447.1; ON762438.1; OL849989.1; OL897126.1; OL896945.1; OL896936.1; OL896931.1; OM233931.1; OM072551.1; OM072822.1; OM296922.1.

Query of SARS-CoV-2 Omicron variant genome which bearing a S protein amino acids sequence in which one of the Omicron-type nucleotide mutation subsets is not mutated and remains the original SARS-CoV-2 Wuhan-Hu-H1-type arrangement. For each of the Omicron variants, BA.1, BA.1.1 and BA.2, the isolates series which bearing a S protein amino acids sequence in which one of the Omicron-type nucleotide mutation subsets is not mutated and remains the original SARS-CoV-2 Wuhan-Hu-H1-type arrangement were named with BA.1-0.1, BA.1.1-0.1 and BA.2-0.1, respectively. In addition, in this article, we named the amino acid sequences of spike protein of BA.1, BA.1.1 and BA.2 as the BA.1_S, BA.1.1_S and BA.2_S, respectively, and then the series of amino acid sequences of spike protein of BA.1-0.1, BA.1.1-0.1 and BA.2-0.1 were named, respectively, as follows; Each Omicron BA.1-0.1 spike series (BA.1-0.1_Ss) were named as BA.1_S:V67A; BA.1_S:69H_70V; BA.1_S:I95T; BA.1_S:D142G_143V_144Y_145Y; BA.1_S:I211N_212L; BA.1_S:ΔEPE; BA.1_S:D339G; BA.1_S:L371S; BA.1_S:P373S; BA.1_S:F375S; BA.1_S:N417K; BA.1_S:K440N; BA.1_S:S446G; BA.1_S:N477S; BA.1_S:K478T; BA.1_S:A484E; BA.1_S:R493Q; BA.1_S:S496G;

BA.1_S:R498Q; BA.1_S:Y501N; BA.1_S:H505Y; BA.1_S:K547T; BA.1_S:G614D; BA.1_S:Y655H; BA.1_S:K679N; BA.1_S:H681P; BA.1_S:K764N; BA.1_S:Y796D; BA.1_S:K856N; BA.1_S:H954Q; BA.1_S:K969N and BA.1_S:F981L / Omicron BA.1.1-0.1 spike series (BA.1.1-0.1_Ss) were named as BA.1.1_S:V67A; BA.1.1_S:69H_70V; BA.1.1_S:I95T; BA.1.1_S:D142G_143V_144Y_145Y; BA.1.1_S:I211N_212L; BA.1.1_S:ΔEPE; BA.1.1_S:D339G; BA.1.1_S:L371S; BA.1.1_S:P373S; BA.1.1_S:F375S; BA.1.1_S:N417K; BA.1.1_S:K440N; BA.1.1_S:S446G; BA.1.1_S:N477S; BA.1.1_S:K478T; BA.1.1_S:A484E; BA.1.1_S:R493Q; BA.1.1_S:S496G; BA.1.1_S:R498Q; BA.1.1_S:Y501N; BA.1.1_S:H505Y; BA.1.1_S:K547T; BA.1.1_S:G614D; BA.1.1_S:Y655H; BA.1.1_S:K679N; BA.1.1_S:H681P; BA.1.1_S:K764N; BA.1.1_S:Y796D; BA.1.1_S:K856N; BA.1.1_S:H954Q; BA.1.1_S:K969N; BA.1.1_S:F981L / Omicron BA.2-0.1 spike series (BA.2-0.1_Ss) were named as BA.2_S:I19T; BA.2_S:24L_25P_26P_S27A; BA.2_S:D142G; BA.2_S:V213G; BA.2_S:D339G; BA.2_S:F371S; BA.2_S:P373S; BA.2_S:F375S; BA.2_S:A376T; BA.2_S:N405D; BA.2_S:S408R; BA.2_S:N417K; BA.2_S:K440N; BA.2_S:N477S; BA.2_S:K478T; BA.2_S:A484E; BA.2_S:R493Q; BA.2_S:R498Q; BA.2_S:Y501N; BA.2_S:H505Y; BA.2_S:G614D; BA.2_S:Y655H; BA.2_S:K679N; BA.2_S:H681P; BA.2_S:K764N; BA.2_S:Y796D; BA.2_S:H954Q; BA.2_S:K969N, and these constructs were showed in Figs. 2, 4 and supplemental Fig 1. These amino acids sequences of spike protein of SARS-CoV-2 Omicron variants, BA.1-0.1, BA.1.1-0.1 and BA.2-0.1 were used as a query sequence for NCBI protein BLAST search. Then the whole genome sequence of BA.1-0.1, BA.1.1-0.1 and BA.2-0.1 isolates bearing the query spike sequence were derived from the BLAST search resultant which identified with query amino acids

sequence with 100%. And then the nucleotide sequences of detected SARS-CoV-2 genome were as follows, GenBank Accession No.: OM117411.1; OP797378.1; OM789835.1; OP928789.1; OP928803.1; OP929381.1; OP929396.1; OP929417.1; OM173977.1; OM518459.1; OM566981.1; ON019560.1; OM097227.1; OM096937.1; OM099902.1; OM117114.1; OM096685.1; OM354436.1; OM646886.1; OM472901.1; OM364511.1; OM131858.1; OL815451.1; OL896986.1; OL897116.1; OL897118.1; OL896964.1; OM367679.1; OM343778.1; OM409228.1; OM396816.1; OM134162.1; OM075886.1; OM123427.1; OM122677.1; OM121681.1; OM224850.1; ON246090.1; OM931599.1; OM864873.1; OM906519.1; OM906587.1; OM464776.1; OM015999.1; OM015958.1; OM015597.1; OM016329.1; OL898806.1; OL898861.1; OM016937.1; OM016186.1; OM036549.1; OM051171.1; OM126493.1; OM079115.1; OM099199.1; OM134489.1; OM098796.1; ON618279.1; ON618009.1; OM627701.1; OM356511.1; OM295457.1; ON700063.1; OM033824.1; ON368355.1; OM084700.1; ON208126.1; OM566593.1; OM945690.2; ON030252.1; ON019844.1; OM890075.1; ON020044.1; OM833954.1; ON376082.1; OM084604.1; OP795273.1; ON066609.1; OM352882.1; OM290510.1; OM369978.1; OM199342.1; OM011974.1; OM090274.1; OM043984.1; OM121683.1; OM121624.1; OM175506.1; OM360429.1; OM360221.1; OM358058.1; OM500517.1; OM135027.1; OM742858.1; OM521685.1; OM896558.1; ON694155.1; OM686755.1; OM484260.1; OM332056.1; OM156397.1; OM079447.1; OM134645.1; OM173298.1; OM123082.1; OM116023.1;

357 OM652943.1; OL994299.1; OL994920.1; OM122027.1; OM121015.1; OL898817.1;

358 OM527504.1; OM225320.1; OM931491.1; OM931575.1; OM931587.1; OM034409.1;

359 OM036283.1; OL996129.1; OM035680.1; OM096996.1; ON065532.1; OM968098.1;

360 OM816604.1; ON235452.1; ON334146.1; OP024162.1; OP209732.1; OM354578.1;

361 OM099080.1; OM297301.1; OM297438.1; OM365368.1; OM449159.1; OM078863.1;

362 OM096959.1; OM117155.1; OM133880.1; OM077358.1; OM372005.1; OM770362.1;

363 OM897488.1; OM918459.1; OM918478.1; OL897115.1; OL897114.1; OL986779.1;

364 OL986696.1; OL987046.1; ON831866.1; OM864099.1; OM863888.1; OP745925.1;

365 ON831672.1; OM043643.1; OM176192.1; OM226685.1; OM343689.1; OM295527.1;

366 OM894975.1; OM846676.1; OM822024.1; OM846844.1; OM906550.1; OM015933.1;

367 OM016323.1; OM016331.1; OM035685.1; OM022498.1; OM156115.1; OM036875.1;

368 OM099560.1; OM199246.1; OM067048.1; OM079299.1; OM099911.1; OM116588.1;

369 OM097010.1; OM173300.1; OM805961.1; OM983266.1; OM983325.1; ON618010.1;

370 OM084691.1; ON021265.1; ON039239.1; ON056981.1; ON144127.1; OM770527.1;

371 OM156164.1; OM155119.1; OM199353.1; OM084630.1; OM084605.1; OM084621.1;

372 OM359369.1; OM411574.1; OM584789.1; OM720486.1; OM429777.1; ON047062.1;

373 ON065416.1; OP415118.1; OM954373.1; ON042406.1; OM335528.1; OM332335.1;

374 OM353626.1; OM332813.1; OM197398.1; OM226919.1; OM228399.1; OM225859.1;

375 OM271353.1; OM159454.1; OM224473.1; OM358278.1; OM361030.1; OM412141.1;

376 OM496298.1; OM044048.1; OM121864.1; OM224477.1; OM227379.1; OM228453.1;

377 OM622156.1; OM906370.1; OM970683.1; ON117965.1; OM198667.1; OM357800.1;

378 OM357161.1; OM335230.1; OM261124.1; OM077578.1; OM497172.1; OM625194.1;

379 OM907131.1; ON047464.1; OM911851.1; OM042846.1; OM155337.1; OM097339.1;

380 OM116805.1; OM134409.1; OM686782.1; OM695863.1; OM724725.1; OM174366.1;

381 OM822132.1; OM822106.1; OM822105.1; OM822485.1; OM135143.1; OM125829.1;

382 OM098855.1; OM156118.1; OM155114.1; OM863926.1; OP359104.1; ON209298.1;

383 ON232806.1; ON421981.1; ON811217.1; OM698275.1; ON052769.1; ON060006.1;

384 ON060007.1; ON060009.1; OM843171.1; OM843276.1; OM843550.1; OM843316.1;

385 OM843340.1; ON049267.1; ON450720.1; ON250163.1; ON256603.1; ON480422.1;

386 OM888844.1; OM890089.1; ON009425.2; ON082904.1; OM901275.1; OM877094.2;

387 OM877095.2; OM877096.2; OM877097.2; ON378542.1; ON389858.1; ON389889.1;

388 ON390359.1; OM936703.1; ON352711.1; ON378000.1; ON177702.1; ON205494.1;

389 ON378633.1; ON617689.1; ON619375.1; OM567618.1; OM659585.1; OM770913.1;

390 OM781641.1; OM533441.1; OM533458.1; OM570235.1; OM570252.1; OM570249.1;

391 OM283361.1; OM283362.1; OM283320.1; OM283343.1; ON618014.1; ON618018.1;

392 ON618019.1; ON618363.1; ON311615.1; ON383919.1; OP579158.1; OP054411.1;

393 ON633107.1; ON414693.1; ON422887.1; OP364296.1; OP629673.1; ON363097.1;

394 OP633561.1; ON458445.1; ON592247.1; ON549687.1; ON067040.1; ON321116.1;

ON199452.1; ON200331.1; OM861064.1; OM969592.1; ON019120.1; ON221861.1; OM861619.1; ON091288.1; ON151370.1; ON233850.1; ON236456.1; ON296711.1; ON535443.1; ON624524.1; ON377450.1; ON397268.1; ON239032.1; ON373649.1; ON481637.1; ON701163.1; ON312677.1; ON349263.1; ON377487.1; ON377609.1; OM638574.1; OM911616.1; OM988767.1; ON019770.1; OM988769.1; ON468158.1; ON608924.1; ON604965.1; ON535763.1; ON378227.1; ON378238.1; ON728470.1.

Query of recombinant SARS-CoV-2 Omicron variant between BA.1 and BA.2 genome

Deduced recombinant spike protein between Omicron variants, BA.1 and BA.2 which showed as the BA.1_S:T19I_L24-_P25-_P26-_A27S_V213G_S371F_T376A_D405N_R408S was used as a query sequence for NCBI protein BLAST search. Then the whole genome sequence of BA.1 and BA.2 recombinant-Omicron isolates bearing some of specific amino acids mutation observed in variant BA.1 and BA.2 in the spike protein region. And then the nucleotide sequences of detected SARS-CoV-2 genome were as follows, GenBank Accession No.: OM360636.1; OM410816.1; OM429902.1; OM497964.1; OM565587.1; OM628132.1; ON549899.1; ON449685.1; ON176765.1; OM628094.1; ON099844.1; OM942313.1; ON395480.1; ON171854.1; ON172005.1; ON076710.1; ON928946.1; OM932113.1; OM942438.1; OM989528.1; OM499181.1; ON414822.1; OM878325.1; ON103067.1; ON103153.1; ON419036.1; ON928719.1; ON337887.1; ON420444.1; ON146520.1; OM469541.1; OM904085.1; ON254531.1; OM881098.1; ON373310.1.

Query of SARS-CoV-2 Omicron variant genome detected in Puerto Rico in 2020

Nucleotide sequences were searched using the keyword PRI PR-UPRRP 2020 (Search details: PRI[All Fields] AND (PR[All Fields] AND UPRRP[All Fields]) AND 2020[All Fields]). And then the search resultants were all SARS-CoV-2 isolate genome sequences. Among these sequences, SARS-CoV-2 Omicron variant related sequences were picked up as follows, GenBank Accession No.: ON928761.1; ON928660.1; ON928794.1; ON928762.1; ON928848.1; ON928741.1; ON928918.1; ON928680.1; ON928975.1; ON928949.1; ON928673.1; ON928865.1; ON928716.1; ON928663.1; ON928779.1; ON928896.1; ON928946.1; ON928912.1; ON928704.1; ON928873.1; ON928813.1; ON928898.1; ON928765.1; ON928912.1; ON928883.1; ON928957.1; ON928880.1; ON928699.1; ON928724.1; ON928941.1.

The genomes were aligned using SnapGene software. Numbering of nucleotide and amino acids number of each protein are provided by using Wuhan-Hu-1 (NC_045512.2; COVID-19/Wuhan-Hu-1CHN/2019/First Isolate) as a reference strain for the definition of mutations.

References

1. F. Wu, S. Zhao, B. Yu, Y. M. Chen, W. Wang, Z. G. Song, Y. Hu, Z. W. Tao, J. H. Tian, Y. Y. Pei, M. L. Yuan, Y. L. Zhang, F. H. Dai, Y. Liu, Q. M. Wang, J. J. Zheng, L. Xu, E. C. Holmes and Y. Z. Zhang: A new coronavirus associated with human respiratory disease in China. *Nature*, 579(7798), 265-269 (2020) doi:10.1038/s41586-020-2008-3
2. R. A. Khailany, M. Safdar and M. Ozaslan: Genomic characterization of a novel SARS-CoV-2. *Gene Rep*, 19, 100682 (2020) doi:10.1016/j.genrep.2020.100682
3. Y. M. Bar-On, A. Flamholz, R. Phillips and R. Milo: SARS-CoV-2 (COVID-19) by the numbers. *Elife*, 9 (2020) doi:10.7554/eLife.57309
4. J. Lan, J. Ge, J. Yu, S. Shan, H. Zhou, S. Fan, Q. Zhang, X. Shi, Q. Wang, L. Zhang and X. Wang: Structure of the SARS-CoV-2 spike receptor-binding domain bound to the ACE2 receptor. *Nature*, 581(7807), 215-220 (2020) doi:10.1038/s41586-020-2180-5
5. D. Wrapp, N. Wang, K. S. Corbett, J. A. Goldsmith, C. L. Hsieh, O. Abiona, B. S. Graham and J. S. McLellan: Cryo-EM structure of the 2019-nCoV spike in the prefusion conformation. *Science*, 367(6483), 1260-1263 (2020) doi:10.1126/science.abb2507
6. B. Korber, W. M. Fischer, S. Gnanakaran, H. Yoon, J. Theiler, W. Abfalterer, N. Hengartner, E. E. Giorgi, T. Bhattacharya, B. Foley, K. M. Hastie, M. D. Parker, D. G. Partridge, C. M. Evans, T. M. Freeman, T. I. de Silva, C.-G. G. Sheffield, C. McDanal, L. G. Perez, H. Tang, A. Moon-Walker, S. P. Whelan, C. C. LaBranche, E. O. Saphire and D. C. Montefiori: Tracking Changes in SARS-CoV-2 Spike: Evidence that D614G Increases Infectivity of the COVID-19 Virus. *Cell*, 182(4), 812-827 e19 (2020) doi:10.1016/j.cell.2020.06.043
7. A. Carrazco-Montalvo, A. Bruno, D. de Mora, M. Olmedo, J. Garces, M. Paez, M. Regato-Arrata, M. Gonzalez, J. Romero, O. Mestanza, B. Freire-Paspuel, A. Gaviria, S. A. Orlando, M. A. Garcia-Bereguiain and L. Patino: First Report of SARS-CoV-2 Lineage B.1.1.7 (Alpha Variant) in Ecuador, January 2021. *Infect Drug Resist*, 14, 5183-5188 (2021) doi:10.2147/IDR.S319439
8. S. Zarate, B. Taboada, J. E. Munoz-Medina, P. Isa, A. Sanchez-Flores, C. Boukadida, A. Herrera-Estrella, N. Selem Mojica, M. Rosales-Rivera, B. Gomez-Gil, A. G. Salas-Lais, C. E. Santacruz-Tinoco, H. Montoya-Fuentes, J. E. Alvarado-Yaah, G. M. Molina-Salinas, G. E. Espinoza-Ayala, J. A. Enciso-Moreno, R. M. Gutierrez-Rios, A. Loza, J. Moreno-Contreras, R. Garcia-Lopez, X. Rivera-Gutierrez, A. Comas-Garcia, R. M. Wong-Chew, M. E. Jimenez-Corona, R. M. Del Angel, J. A. Vazquez-Perez, M. Matias-Florentino, M. Perez-Garcia, S. Avila-Rios, H. G. Castelan-Sanchez, L. Delaye, L. P. Martinez-Castilla, M. Escalera-Zamudio, S. Lopez and C. F. Arias: The Alpha Variant (B.1.1.7) of SARS-CoV-2 Failed to Become Dominant in Mexico. *Microbiol Spectr*, 10(2), e0224021 (2022) doi:10.1128/spectrum.02240-21
9. H. Tegally, E. Wilkinson, M. Giovanetti, A. Iranzadeh, V. Fonseca, J. Giandhari, D. Doolabh, S. Pillay, E. J. San, N. Msomi, K. Mlisana, A. von Gottberg, S. Walaza, M. Allam, A. Ismail, T. Mohale, A. J. Glass, S. Engelbrecht, G. Van Zyl, W. Preiser, F. Petruccione, A. Sigal, D. Hardie, G. Marais, N.-y. Hsiao, S. Korsman, M.-A. Davies, L. Tyers, I. Mudau, D. York, C. Maslo, D. Goedhals, S. Abrahams, O. Laguda-Akingba, A. Alisoltani-Dehkordi, A. Godzik, C. K. Wibmer, B. T. Sewell, J. Lourenço, L. C. J. Alcantara, S. L. Kosakovsky Pond, S. Weaver, D. Martin, R. J. Lessells, J. N.

Bhiman, C. Williamson and T. de Oliveira: Detection of a SARS-CoV-2 variant of concern in South Africa. *Nature*, 592(7854), 438-443 (2021) doi:10.1038/s41586-021-03402-9

10. T. Fujino, H. Nomoto, S. Kutsuna, M. Ujiie, T. Suzuki, R. Sato, T. Fujimoto, M. Kuroda, T. Wakita and N. Ohmagari: Novel SARS-CoV-2 Variant in Travelers from Brazil to Japan. *Emerg Infect Dis*, 27(4), 1243-5 (2021) doi:10.3201/eid2704.210138

11. M. Joshi, M. Kumar, V. Srivastava, D. Kumar, D. S. Rathore, R. Pandit, D. W. Graham and C. G. Joshi: Genetic sequencing detected the SARS-CoV-2 delta variant in wastewater a month prior to the first COVID-19 case in Ahmedabad (India). *Environ Pollut*, 310, 119757 (2022) doi:10.1016/j.envpol.2022.119757

12. K. Laiton-Donato, C. Franco-Munoz, D. A. Alvarez-Diaz, H. A. Ruiz-Moreno, J. A. Usme-Ciro, D. A. Prada, J. Reales-Gonzalez, S. Corchuelo, M. T. Herrera-Sepulveda, J. Naizaque, G. Santamaria, J. Rivera, P. Rojas, J. H. Ortiz, A. Cardona, D. Malo, F. Prieto-Alvarado, F. R. Gomez, M. Wiesner, M. L. O. Martinez and M. Mercado-Reyes: Characterization of the emerging B.1.621 variant of interest of SARS-CoV-2. *Infect Genet Evol*, 95, 105038 (2021) doi:10.1016/j.meegid.2021.105038

13. J. Quarleri, V. Galvan and M. V. Delpino: Omicron variant of the SARS-CoV-2: a quest to define the consequences of its high mutational load. *Geroscience*, 44(1), 53-56 (2022) doi:10.1007/s11357-021-00500-4

14. A. Gowrisankar, T. M. C. Priyanka and S. Banerjee: Omicron: a mysterious variant of concern. *Eur Phys J Plus*, 137(1), 100 (2022) doi:10.1140/epjp/s13360-021-02321-y

15. A. Vitiello, F. Ferrara, A. M. Auti, M. Di Domenico and M. Boccellino: Advances in the Omicron variant development. *J Intern Med*, 292(1), 81-90 (2022) doi:10.1111/joim.13478

16. Y. Fan, X. Li, L. Zhang, S. Wan, L. Zhang and F. Zhou: SARS-CoV-2 Omicron variant: recent progress and future perspectives. *Signal Transduct Target Ther*, 7(1), 141 (2022) doi:10.1038/s41392-022-00997-x

17. J. Fonager, M. Bennedbaek, P. Bager, J. Wohlfahrt, K. M. Ellegaard, A. C. Ingham, S. M. Edslev, M. Stegger, R. N. Sieber, R. Lassauniere, A. Fomsgaard, T. Lillebaek, C. W. Svarrer, F. T. Moller, C. H. Moller, R. Legarth, T. V. Sydenham, K. Steinke, S. J. Paulsen, J. A. S. Castruita, U. V. Schneider, C. H. Schouw, X. C. Nielsen, M. Overvad, R. T. Nielsen, R. L. Marvig, M. S. Pedersen, L. Nielsen, L. L. Nilsson, J. Bybjerg-Grauholm, I. H. Tarpgaard, T. S. Ebsen, J. U. H. Lam, V. Gunalan and M. Rasmussen: Molecular epidemiology of the SARS-CoV-2 variant Omicron BA.2 sub-lineage in Denmark, 29 November 2021 to 2 January 2022. *Euro Surveill*, 27(10) (2022) doi:10.2807/1560-7917.ES.2022.27.10.2200181

18. L. B. Shrestha, C. Foster, W. Rawlinson, N. Tedla and R. A. Bull: Evolution of the SARS-CoV-2 omicron variants BA.1 to BA.5: Implications for immune escape and transmission. *Rev Med Virol*, 32(5), e2381 (2022) doi:10.1002/rmv.2381

19. L. Yao, K. L. Zhu, X. L. Jiang, X. J. Wang, B. D. Zhan, H. X. Gao, X. Y. Geng, L. J. Duan, E. H. Dai and M. J. Ma: Omicron subvariants escape antibodies elicited by vaccination and BA.2.2 infection. *Lancet Infect Dis*, 22(8), 1116-1117 (2022) doi:10.1016/S1473-3099(22)00410-8

20. S. Torii, C. Ono, R. Suzuki, Y. Morioka, I. Anzai, Y. Fauzyah, Y. Maeda, W. Kamitani, T. Fukuhara and Y. Matsuura: Establishment of a reverse genetics system for SARS-CoV-2 using circular polymerase extension reaction. *Cell Rep*, 35(3), 109014 (2021) doi:10.1016/j.celrep.2021.109014

21. T. Y. Taha, I. P. Chen, J. M. Hayashi, T. Tabata, K. Walcott, G. R. Kimmerly, A. M. Syed, A. Ciling, R. K. Suryawanshi, H. S. Martin, B. H. Bach, C. L. Tsou, M. Montano, M. M. Khalid, B. K. Sreekumar, G. Renuka Kumar, S. Wyman, J. A. Doudna and M. Ott: Rapid assembly of SARS-CoV-2 genomes reveals attenuation of the Omicron BA.1 variant through NSP6. *Nat Commun*, 14(1), 2308 (2023) doi:10.1038/s41467-023-37787-0

22. W. Wang, X. Peng, Y. Jin, J. A. Pan and D. Guo: Reverse genetics systems for SARS-CoV-2. *J Med Virol*, 94(7), 3017-3031 (2022) doi:10.1002/jmv.27738

23. L. Xu, L. Bao, Q. Lv, W. Deng, Y. Ma, F. Li, L. Zhan, H. Zhu, C. Ma and C. Qin: A single-amino-acid substitution in the HA protein changes the replication and pathogenicity of the 2009 pandemic A (H1N1) influenza viruses in vitro and in vivo. *Virol J*, 7, 325 (2010) doi:10.1186/1743-422X-7-325

24. L. A. Silva, S. Khomandiak, A. W. Ashbrook, R. Weller, M. T. Heise, T. E. Morrison and T. S. Dermody: A single-amino-acid polymorphism in Chikungunya virus E2 glycoprotein influences glycosaminoglycan utilization. *J Virol*, 88(5), 2385-97 (2014) doi:10.1128/JVI.03116-13

25. K. A. Tsetsarkin, D. L. Vanlandingham, C. E. McGee and S. Higgs: A single mutation in chikungunya virus affects vector specificity and epidemic potential. *PLoS Pathog*, 3(12), e201 (2007) doi:10.1371/journal.ppat.0030201

26. X. C. Tang, S. S. Agnihothram, Y. Jiao, J. Stanhope, R. L. Graham, E. C. Peterson, Y. Avnir, A. S. Tallarico, J. Sheehan, Q. Zhu, R. S. Baric and W. A. Marasco: Identification of human neutralizing antibodies against MERS-CoV and their role in virus adaptive evolution. *Proc Natl Acad Sci U S A*, 111(19), E2018-26 (2014) doi:10.1073/pnas.1402074111

27. J. Sui, D. R. Aird, A. Tamin, A. Murakami, M. Yan, A. Yammanuru, H. Jing, B. Kan, X. Liu, Q. Zhu, Q. A. Yuan, G. P. Adams, W. J. Bellini, J. Xu, L. J. Anderson and W. A. Marasco: Broadening of neutralization activity to directly block a dominant antibody-driven SARS-coronavirus evolution pathway. *PLoS Pathog*, 4(11), e1000197 (2008) doi:10.1371/journal.ppat.1000197

28. J. ter Meulen, E. N. van den Brink, L. L. Poon, W. E. Marissen, C. S. Leung, F. Cox, C. Y. Cheung, A. Q. Bakker, J. A. Bogaards, E. van Deventer, W. Preiser, H. W. Doerr, V. T. Chow, J. de Kruif, J. S. Peiris and J. Goudsmit: Human monoclonal antibody combination against SARS coronavirus: synergy and coverage of escape mutants. *PLoS Med*, 3(7), e237 (2006) doi:10.1371/journal.pmed.0030237

29. L. van Dorp, D. Richard, C. C. S. Tan, L. P. Shaw, M. Acman and F. Balloux: No evidence for increased transmissibility from recurrent mutations in SARS-CoV-2. *Nat Commun*, 11(1), 5986 (2020) doi:10.1038/s41467-020-19818-2

Competing interests

The authors declare no competing interests.

Figure legends

Fig. 1. Mutation subsets of S protein of SARS-CoV-2 variants.

Sequence of S protein of SARS-CoV-2 variants（variants of concerns: VOCs; Alpha:B.1.1.7, Beta:B.1.351, Gamma:P1, Delta:B.1.617.2.63, and Omicron:BA.1; BA.2 and variants of interest: VOIs; Lambda:C.37, Mu:B.1.621) are compared with that of the SARS-CoV-2 Wuhan-Hu-H1 reference sequence, and extracted the different amino acids (amino acids change, deletion, and insertion) and synonymous changes of nucleotides are shown. Non-synonymous changes are shown by amino acid changes (capital letters), and synonymous changes are shown by nucleotide changes (small letters). Amino acids different from Wuhan-Hu-H1 found in each variant, Alpha: B.1.1.7, Beta: B.1.351, Gamma: P1, Delta: B.1.617.2.63, Lambda: C.37, Mu: B.1.621, Omicron: BA.1, BA.2 are highlighted with red, orange, green, yellow, aquamarine, lime, deep sky blue, and blue violet, respectively. Amino acid changes common to Omicron: BA.1 and BA.2 are shown in purple.

Fig. 2. Mutations of S proteins of SARS-CoV-2 Omicron isolates.

(A) Different amino acids and synonymous change of nucleotides in **S** proteins of SARS-CoV-2 Omicron BA.1, BA.1.1 isolates and BA.1-0.1s compared to that of SARS-CoV-2 Wuhan-Hu-H1. Nucleotide deletions and insertions those were "deletion^{1}" (deletion: nt 21,766-21,771), "deletion^{2}" (deletion: nt 21,987-21,995), "deletion^{3}" (deletion: nt 22,194-22,196), and "insertion^{4}" (insertion between 22,206-22,196), introduced the amino acids changes H69-_V70-, G142D_V143-_Y144-_Y145-, N211I_L212- and 215ins.EPE, respectively. (B) Different amino acids and synonymous nucleotide change in S proteins in SARS-CoV-2 Omicron BA.1.1-

0.1 isolates. Amino acids different from Wuhan-Hu-H1 found in each variant, Alpha: B.1.1.7, Beta: B.1.351, Gamma: P1, Delta: B.1.617.2.63, Mu: B.1.621, Omicron: BA.1, BA.2 are highlighted with red, orange, green, yellow, lime, deep sky blue, and blue violet, respectively. Amino acid changes common to Omicron:BA.1 and BA.2 are highlighted with purple.

Fig. 3. Estimated homologous recombination breakpoints of the SARS-CoV-2 S gene of Omicron BA.1-0.1 or BA.1.1-0.1

Sequence alignment of the amino acids and their coding nucleotides (nt.21,746-21,787; nt.22,658-22,702; nt.22,976-23,011 and nt.23,582-23,620) containing the mutation point of SARS-CoV-2 S gene of Omicron BA.1 variant compared to that of SARS-CoV-2 Wuhan-Hu-H1. Changed nucleotides and amino acids of Omicron BA.1 are shown in red letters. Estimated homologous recombination breakpoints of the SARS-CoV-2 S gene of Omicron BA.1-0.1 or BA.1.1-0.1 are shown by asterisks.

Fig. 4. Representative mutations of SARS-CoV-2 Omicron isolates other than S protein.

(A) Representative amino acids and synonymous changes of nucleotides of SARS-CoV-2 Omicron BA.1, BA.1.1 isolates, and BA.1-0.1 compared to SARS-CoV-2 Wuhan-Hu-H1. **(B)** Representative amino acids and synonymous changes of nucleotides of SARS-CoV-2 Omicron BA.1.1-0.1 compared to SARS-CoV-2 Wuhan-Hu-H1. Amino acids different from Wuhan-Hu-H1 found in each variant, Alpha: B.1.1.7, Lambda: C.37, Mu: B.1.621, Omicron: BA.1 are highlighted with red, aquamarine, deep sky blue, and blue violet, respectively.

574 Amino acid changes common to Omicron: BA.1 and BA.2 are shown in purple. Synonymous nucleotide
575 changes, c2470u observed in Omicron:BA.1.1 mainly shown with blue. Synonymous and non-synonymous
576 changes, u10135c of nsp5, L106F in ORF3, and D343G in N protein that subset observed ~40% of Omicron:
577 BA.1-0.1 are highlighted with emerald-green. Undetermined nucleotide(s) or amino acid(s) are shown as UD
578 or X, respectively.
579
580 **Fig. 5. Mutations of the S proteins of SARS-CoV-2 Omicron BA.1-BA.2 recombinant isolates and SARS-**
581 **CoV-2 Omicron BA.1 and BA.2 isolates detected in Puerto Rico in 2020.**
582 **(A)** Different amino acids and synonymous change of nucleotides in S proteins of SARS-CoV-2 Omicron BA.1-
583 BA.2 recombinant isolates compared to that of SARS-CoV-2 Wuhan-Hu-H1. Nucleotide deletions, "deletion^{5}"
584 (deletion: nt 21,633-21,641), introduced the amino acids changes L24-_P25-_P26-_A27S. **(B)** Different amino
585 acids and synonymous change of nucleotides in S proteins of SARS-CoV-2 Omicron BA.1.1, Omicron BA.1-
586 BA.2 recombinant isolate, which is highlighted with magenta (GenBank: ON928946.1), Omicron BA.2 and
587 Omicron 2-0.1(K440N) those detected in Puerto Rico in 2020. Amino acids different from Wuhan-Hu-H1 found
588 in each variant, Alpha: B.1.1.7, Beta: B.1.351, Gamma: P1, Delta: B.1.617.2.63, Mu: B.1.621, Omicron: BA.1,
589 BA.2 are highlighted with red, orange, green, yellow, lime, deep sky blue, and blue-violet, respectively. Amino
590 acid changes common to Omicron: BA.1 and BA.2 are highlighted with purple.

Supplemental Figure 1

Human coronavirus 229E strains which detected in Seattle, USA, in 2015 and 2019.

Alignment of nucleotide **(A)** and amino acid **(B)** sequences of S region of Human coronavirus 229E strains, HCoV_229E/Seattle/USA/SC3112/2015 (GenBank: KY983587.1) and CoV_229E/Seattle/USA/SC0865/2019 (GenBank: MN306046.1). The number of nucleotide substitutions observed between them was 32 and amino acid substitutions were 18 between them, and synonymous (14: 32-18)–non-synonymous mutation (18) rates between them was 1.285

Supplemental Figure 2

Different amino acids and synonymous change of nucleotides in S proteins of SARS-CoV-2 Omicron BA.2 isolates and BA.2-0.1s those compared to that of SARS-CoV-2 Wuhan-Hu-H1.

Nucleotide deletions, "deletion^{5}" (deletion: nt 21,633-21,641), introduced the amino acids changes L24-_P25-_P26-_A27S. Amino acids different from Wuhan-Hu-H1 found in each variant, Alpha: B.1.1.7, Beta: B.1.351, Gamma: P1, Delta: B.1.617.2.63, Mu: B.1.621, Omicron: BA.1, BA.2 are highlighted with red, orange, green, yellow, lime, deep sky blue, and blue-violet, respectively. Amino acid changes common to Omicron: BA.1 and BA.2 are highlighted with purple.

Supplemental Figure 3 Estimated homologous recombination breakpoints of the SARS-CoV-2 S gene of Omicron BA.2-0.1 or BA.1-BA.2 recombinant.

610 **(A)** Sequence alignment of the amino acids and its coding nucleotides (nt. 22,658-22,702) containing the
611 mutation point of SARS-CoV-2 S gene of Omicron BA.2 variants compared to that of SARS-CoV-2 Wuhan-
612 Hu-H1. **(B)** Sequence alignment of the amino acids and its coding nucleotides (nt. 22,178-22,222) containing
613 the mutation point of SARS-CoV-2 S gene of Omicron BA,1, BA.2 variant and BA.1-BA.2 recombinant
614 isolate compared to that of SARS-CoV-2 Wuhan-Hu-H1. Changed nucleotides and amino acids of Omicron
615 variants BA.1, BA.2, and BA.1-BA.2 recombinant isolate compared to that of SARS-CoV-2 Wuhan-Hu-H1
616 sequences are shown in red letters. Asterisks showed an estimated homologous recombination breakpoint of
617 the SARS-CoV-2 S gene of Omicron BA.2-0.1.
618

Fig. 1

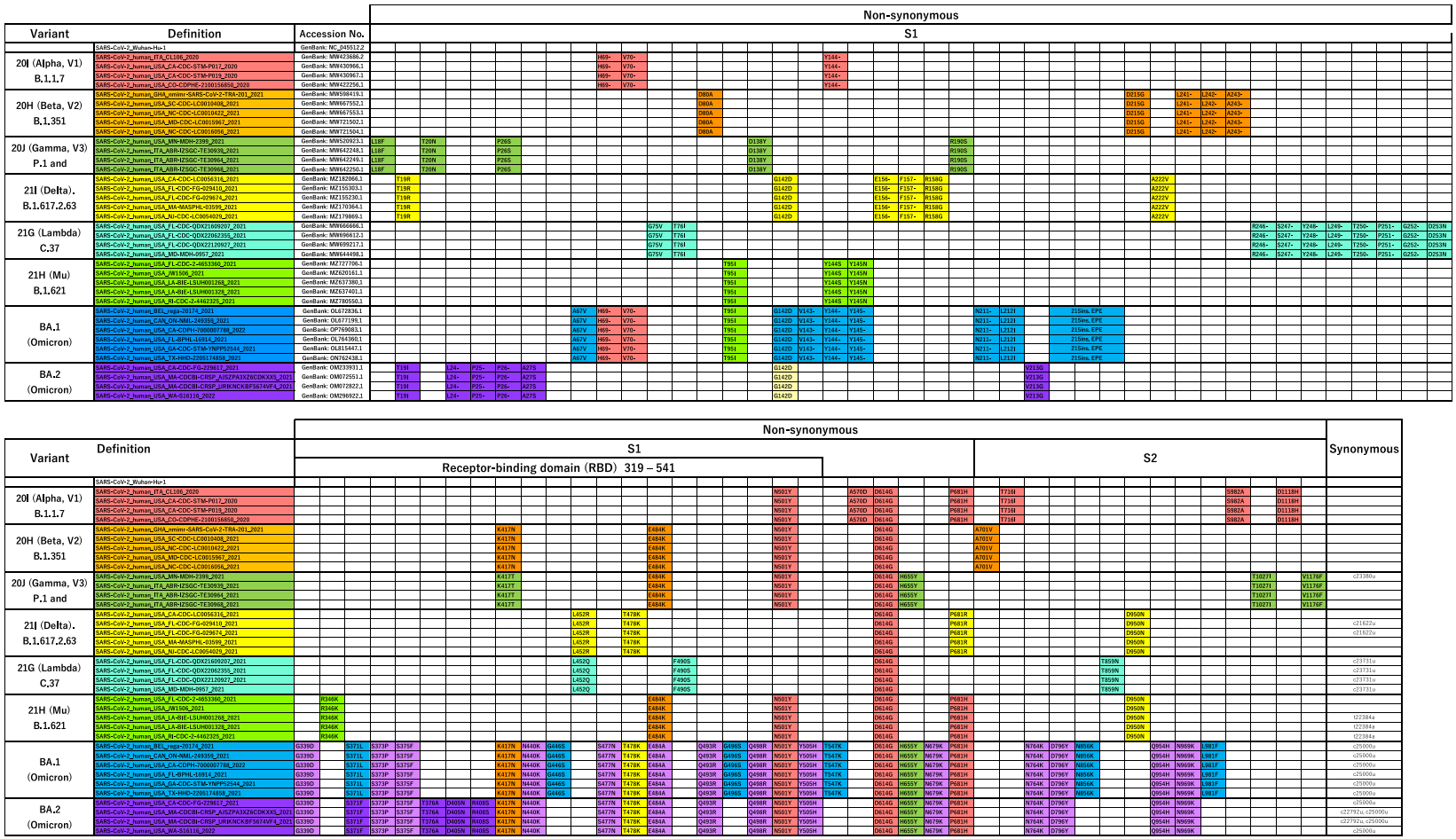
Non-synonymous
S1
Variant
Definition
Accession No.
20I (Alpha, V1) B.1.1.7
20H (Beta, V2) B.1.351
20J (Gamma, V3) P.1 and
21I (Delta), B.1.617.2.63
21G (Lambda) C.37
21H (Mu) B.1.621
BA.1 (Omicron)
BA.2 (Omicron)
Non-synonymous
S1
Receptor-binding domain (RBD) 319 – 541
S2
Synonymous
Variant
Definition

Fig. 2 A

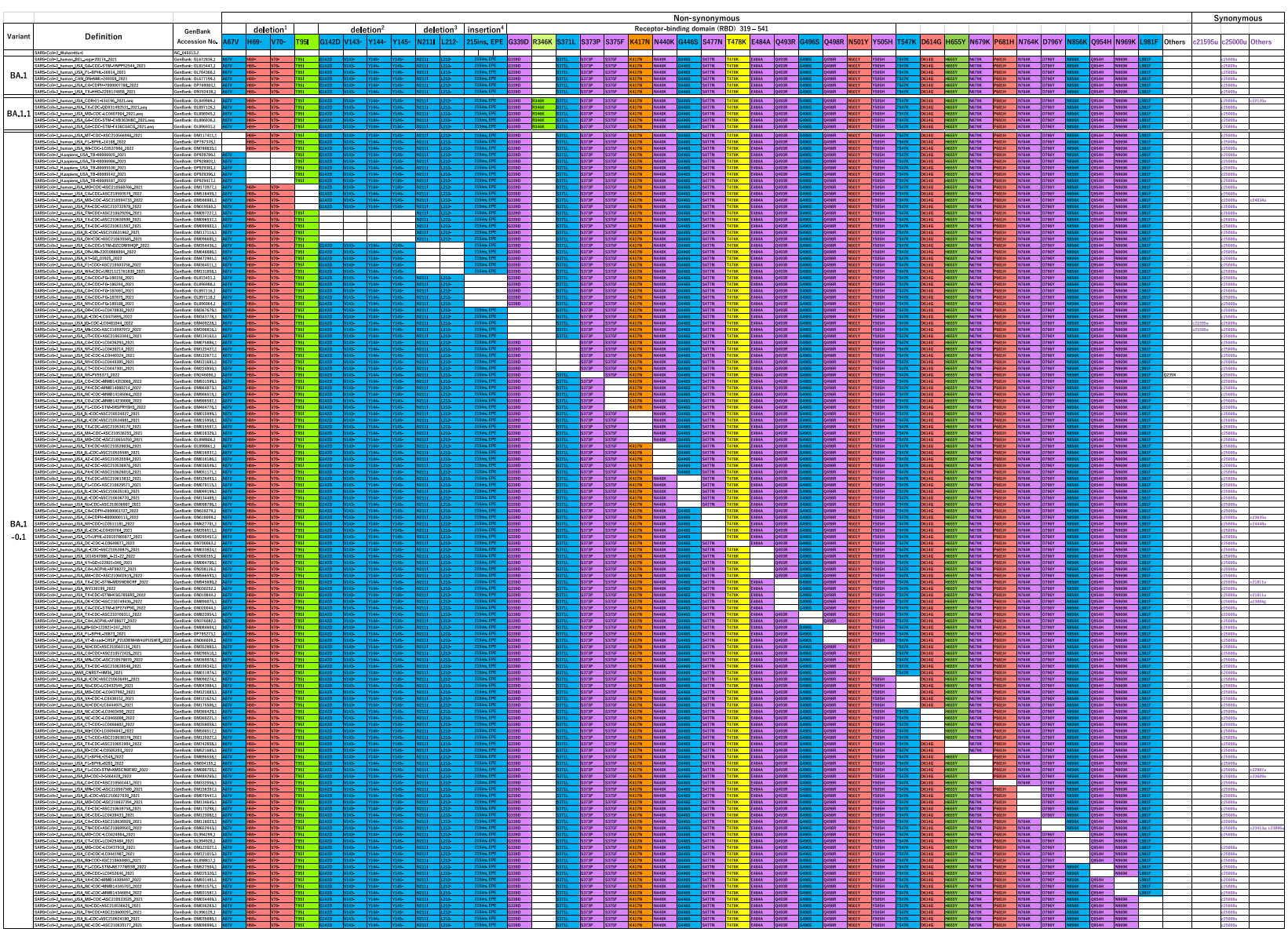

Fig. 2 B

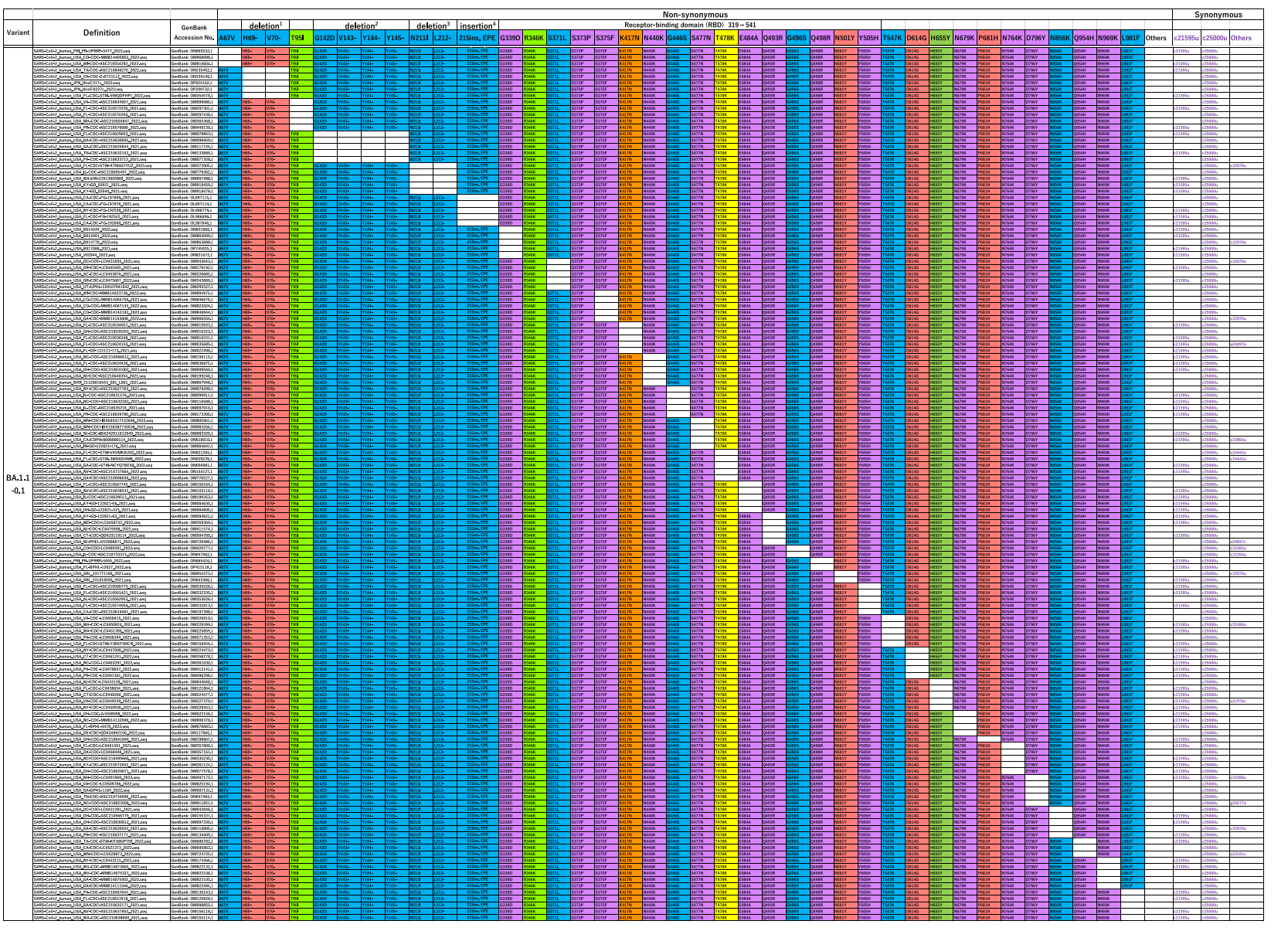

Fig. 3

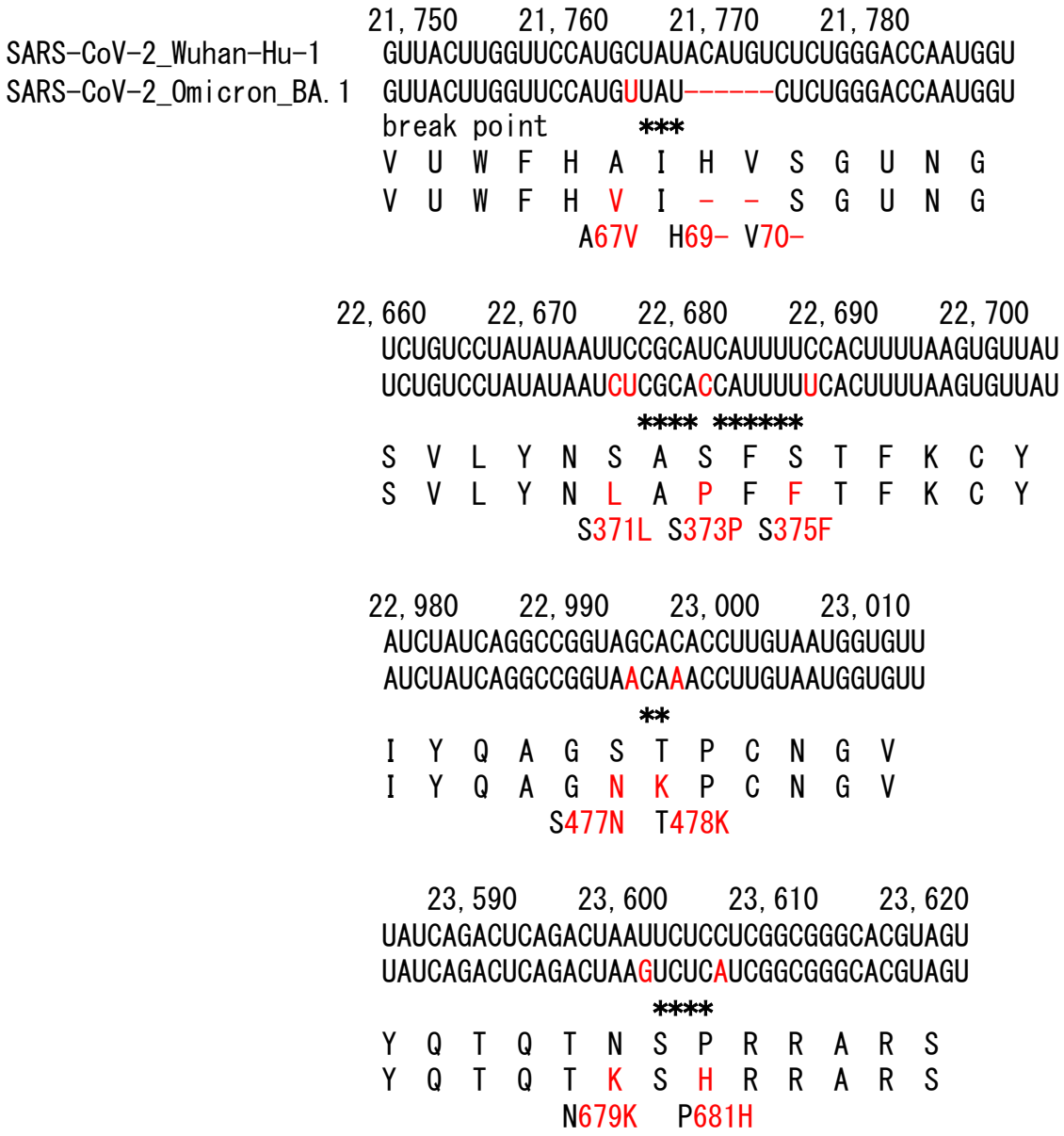
21,750 21,760 21,770 21,780
SARS-CoV-2_Wuhan-Hu-1 GUUACUUGGUUCCAUGCUAUACAUGUCUCUGGGACCAAUGGU
SARS-CoV-2_Omicron_BA.1 GUUACUUGGUUCCAUGUUAU------CUCUGGGACCAAUGGU
break point ***
V U W F H A I H V S G U N G
V U W F H V I - - S G U N G
A67V H69- V70-
22,660 22,670 22,680 22,690 22,700
UCUGUCCUAUAUAAUUCCGCAUCAUUUUCCACUUUUAAGUGUUAU
UCUGUCCUAUAUAAUCUCGCACCAUUUUUCACUUUUAAGUGUUAU
**** ******
S V L Y N S A S F S T F K C Y
S V L Y N L A P F F T F K C Y
S371L S373P S375F
22,980 22,990 23,000 23,010
AUCUAUCAGGCCGGUAGCACACCUUGUAAUGGUGUU
AUCUAUCAGGCCGGUAACAACCUUGUAAUGGUGUU
**
I Y Q A G S T P C N G V
I Y Q A G N K P C N G V
S477N T478K
23,590 23,600 23,610 23,620
UAUCAGACUCAGACUAAUUCUCCUCGGCGGGCACGUAGU
UAUCAGACUCAGACUAAGUCUCAUCGGCGGGCACGUAGU
****
Y Q T Q T N S P R R A R S
Y Q T Q T K S H R R A R S
N679K P681H

Fig. 4 A

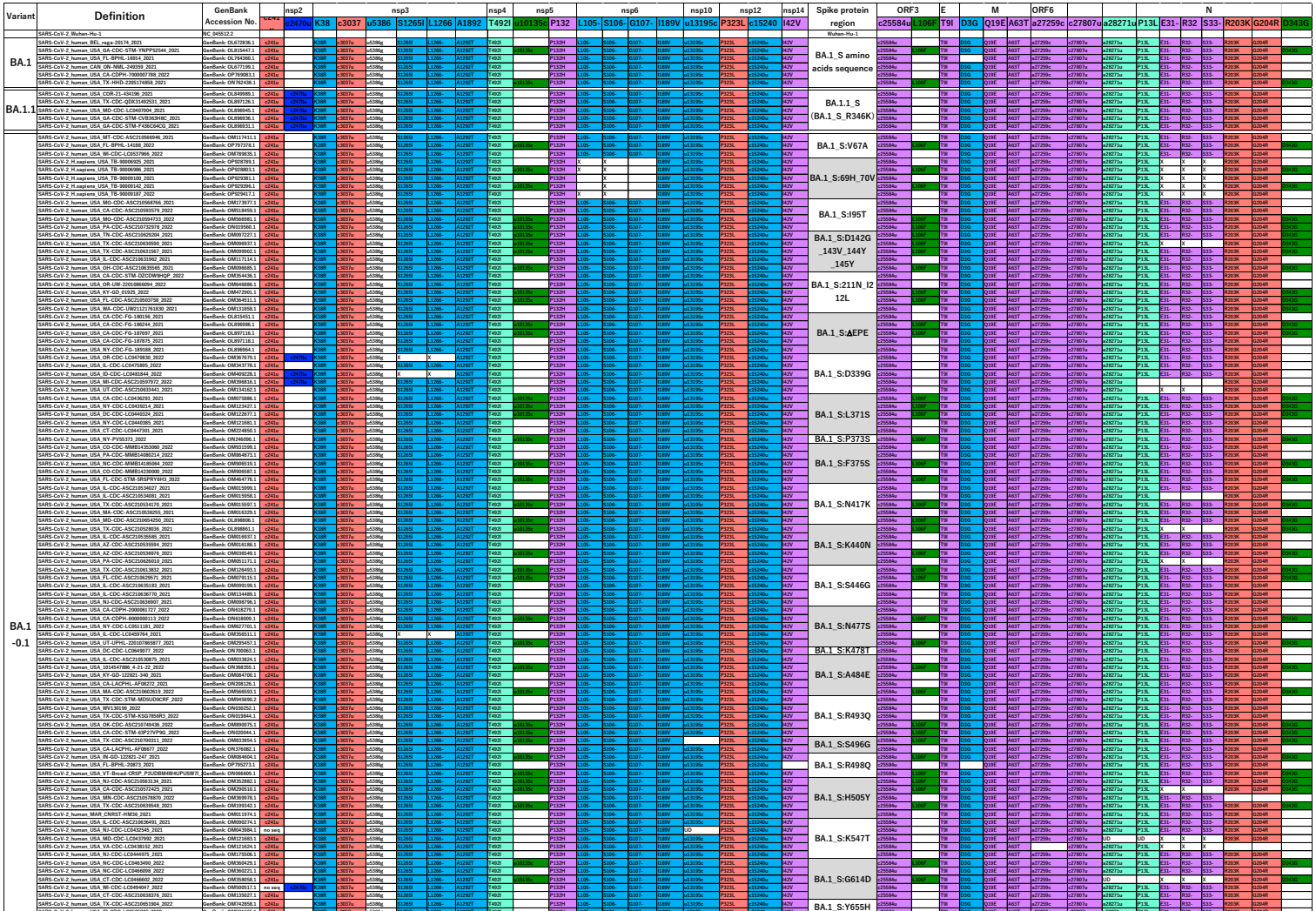

Fig. 4 B

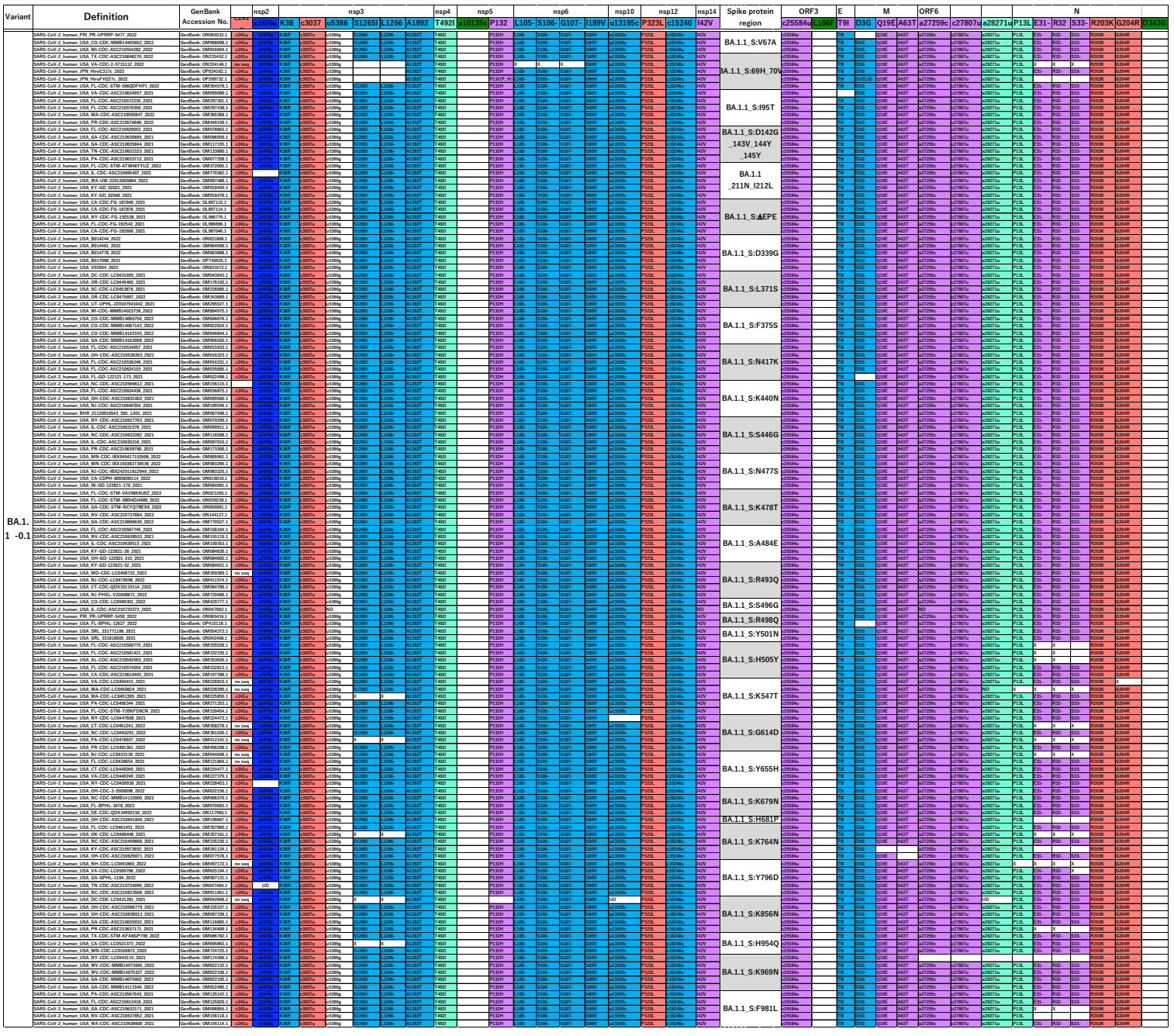

Fig. 5

A

SARS-CoV-2_Omicron_BA1-BA2 recombinant (BA1/2)

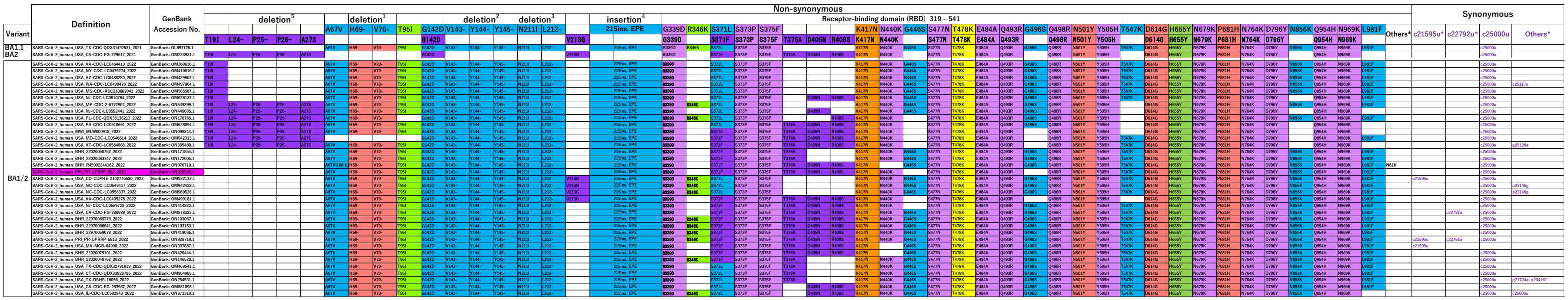

B

SARS-CoV-2_isolated in Puerto Rico in 2020

Supplemental Figure 1

A

B

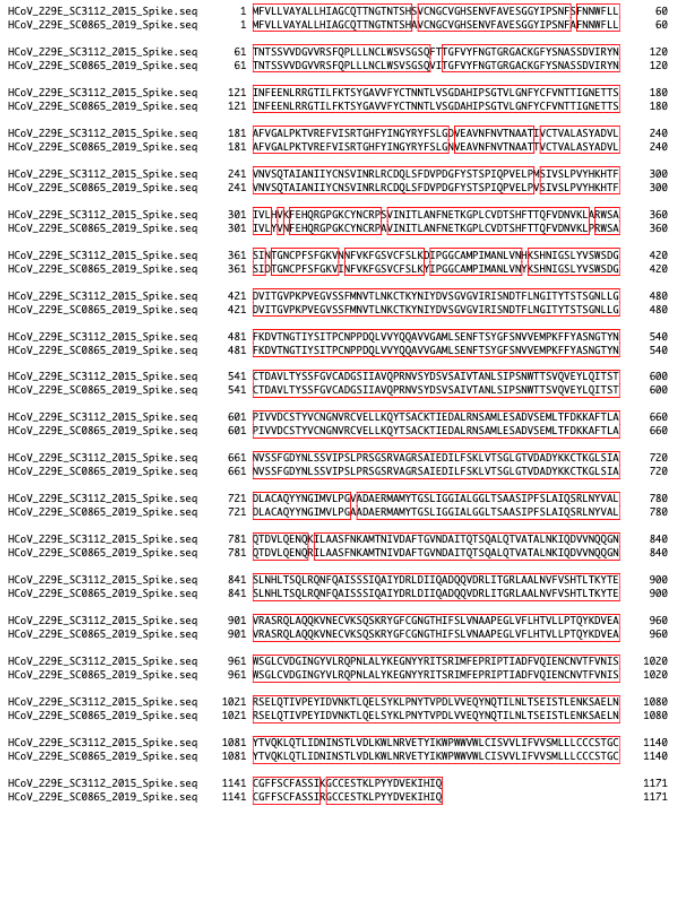

Supplemental Figure 2

			Non-synonymous																																Synonymous		
				deletion						Receptor-binding domain (RBD) 319 – 541																										
Variant	Definition	GenBank Accession No.	T19I	L24-	P25-	P26-	A27S	G142D	V213G	G339D	S371F	S373P	S375F	T376A	D405N	R408S	K417N	N440K	S477N	T478K	E484A	Q493R	Q498R	N501Y	Y505H	D614G	H655Y	N679K	P681H	N764K	D796Y	Q954H	N969K	c22792u*	c25000u	Ouhers*
BA.2	SARS-CoV-2_human_USA_CA-CDC-FG-229617_2021	GenBank: OM233931.1	T19I	L24-	P25-	P26-	A27S	G142D	V213G	G339D	S371F	S373P	S375F	T376A	D405N	R408S	K417N	N440K	S477N	T478K	E484A	Q493R	Q498R	N501Y	Y505H	D614G	H655Y	N679K	P681H	N764K	D796Y	Q954H	N969K		c25000u	
	SARS-CoV-2_human_USA_MA-CDCBI-CRSP_AJSZPA3XZ6CDKXX5_2021	GenBank: OM072551.1	T19I	L24-	P25-	P26-	A27S	G142D	V213G	G339D	S371F	S373P	S375F	T376A	D405N	R408S	K417N	N440K	S477N	T478K	E484A	Q493R	Q498R	N501Y	Y505H	D614G	H655Y	N679K	P681H	N764K	D796Y	Q954H	N969K	c22792u	c25000u	
	SARS-CoV-2_human_USA_MA-CDCBI-CRSP_URIKNCKBF5674VF4_2021	GenBank: OM072822.1	T19I	L24-	P25-	P26-	A27S	G142D	V213G	G339D	S371F	S373P	S375F	T376A	D405N	R408S	K417N	N440K	S477N	T478K	E484A	Q493R	Q498R	N501Y	Y505H	D614G	H655Y	N679K	P681H	N764K	D796Y	Q954H	N969K	c22792u	c25000u	
	SARS-CoV-2_human_USA_WA-S16116_2022	GenBank: OM296922.1	T19I	L24-	P25-	P26-	A27S	G142D	V213G	G339D	S371F	S373P	S375F	T376A	D405N	R408S	K417N	N440K	S477N	T478K	E484A	Q493R	Q498R	N501Y	Y505H	D614G	H655Y	N679K	P681H	N764K	D796Y	Q954H	N969K		c25000u	
BA.2.-0.1	SARS-CoV-2_human_USA_B015025_2022	GenBank: OM863926.1		L24-	P25-	P26-	A27S	G142D	V213G	G339D	S371F	S373P	S375F	T376A	D405N	R408S	K417N	N440K	S477N	T478K	E484A	Q493R	Q498R	N501Y	Y505H	D614G	H655Y	N679K	P681H	N764K	D796Y	Q954H	N969K		c25000u	
	SARS-CoV-2_human_USA_CA-CCPHL-2023_2022	GenBank: ON209298.1		L24-	P25-	P26-	A27S	G142D	V213G	G339D	S371F	S373P	S375F	T376A	D405N	R408S	K417N	N440K	S477N	T478K	E484A	Q493R	Q498R	N501Y	Y505H	D614G	H655Y	N679K	P681H	N764K	D796Y	Q954H	N969K	c22792u	c25000u	a22948g
	SARS-CoV-2_human_USA_CA-CDC-LC0569601_2022	GenBank: ON232806.1		L24-	P25-	P26-	A27S	G142D	V213G	G339D	S371F	S373P	S375F	T376A	D405N	R408S	K417N	N440K	S477N	T478K	E484A	Q493R	Q498R	N501Y	Y505H	D614G	H655Y	N679K	P681H	N764K	D796Y	Q954H	N969K		c25000u	
	SARS-CoV-2_human_USA_CA-LACPHL-AF08976_2022	GenBank: ON421981.1		L24-	P25-	P26-	A27S	G142D	V213G	G339D	S371F	S373P	S375F	T376A	D405N	R408S	K417N	N440K	S477N	T478K	E484A	Q493R	Q498R	N501Y	Y505H	D614G	H655Y	N679K	P681H	N764K	D796Y	Q954H	N969K		c25000u	
	SARS-CoV-2_human_USA_CA-LACPHL-AF10606_2022	GenBank: ON811217.1		L24-	P25-	P26-	A27S	G142D	V213G	G339D	S371F	S373P	S375F	T376A	D405N	R408S	K417N	N440K	S477N	T478K	E484A	Q493R	Q498R	N501Y	Y505H	D614G	H655Y	N679K	P681H	N764K	D796Y	Q954H	N969K		c25000u	
	SARS-CoV-2_human_USA_NY-CDC-LC0518422_2022	GenBank: OM698275.1	T19I					G142D	V213G	G339D	S371F	S373P	S375F	T376A	D405N	R408S	K417N	N440K	S477N	T478K	E484A	Q493R	Q498R	N501Y	Y505H	D614G	H655Y	N679K	P681H	N764K	D796Y	Q954H	N969K		c25000u	c23635u
	SARS-CoV-2_human_IND_17_2021	GenBank: ON052769.1	T19I					G142D	V213G	G339D	S371F	S373P	S375F	T376A	D405N	R408S	K417N	N440K	S477N	T478K	E484A	Q493R	Q498R	N501Y	Y505H	D614G	H655Y	N679K	P681H	N764K	D796Y	Q954H	N969K		c25000u	
	SARS-CoV-2_human_IND_LNHD132_2022	GenBank: ON060006.1	T19I					G142D	V213G	G339D	S371F	S373P	S375F	T376A	D405N	R408S	K417N	N440K	S477N	T478K	E484A	Q493R	Q498R	N501Y	Y505H	D614G	H655Y	N679K	P681H	N764K	D796Y	Q954H	N969K		c25000u	
	SARS-CoV-2_human_IND_LNHD133_2022	GenBank: ON060007.1	T19I					G142D	V213G	G339D	S371F	S373P	S375F	T376A	D405N	R408S	K417N	N440K	S477N	T478K	E484A	Q493R	Q498R	N501Y	Y505H	D614G	H655Y	N679K	P681H	N764K	D796Y	Q954H	N969K		c25000u	
	SARS-CoV-2_human_IND_LNHD135_2022	GenBank: ON060009.1	T19I					G142D	V213G	G339D	S371F	S373P	S375F	T376A	D405N	R408S	K417N	N440K	S477N	T478K	E484A	Q493R	Q498R	N501Y	Y505H	D614G	H655Y	N679K	P681H	N764K	D796Y	Q954H	N969K		c25000u	
	SARS-CoV-2_human_BHR_22020069673_S64_L001_2022	GenBank: OM843171.1	T19I	L24-	P25-	P26-	A27S		V213G	G339D	S371F	S373P	S375F	T376A	D405N	R408S	K417N	N440K	S477N	T478K	E484A	Q493R	Q498R	N501Y	Y505H	D614G	H655Y	N679K	P681H	N764K	D796Y	Q954H	N969K			
	SARS-CoV-2_human_BHR_22020087657_S183_L001_2022	GenBank: OM843276.1	T19I	L24-	P25-	P26-	A27S		V213G	G339D	S371F	S373P	S375F	T376A	D405N	R408S	K417N	N440K	S477N	T478K	E484A	Q493R	Q498R	N501Y	Y505H	D614G	H655Y	N679K	P681H	N764K	D796Y	Q954H	N969K			
	SARS-CoV-2_human_BHR_R1222690028093_S242_L001_2022	GenBank: OM843550.1	T19I	L24-	P25-	P26-	A27S		V213G	G339D	S371F	S373P	S375F	T376A	D405N	R408S	K417N	N440K	S477N	T478K	E484A	Q493R	Q498R	N501Y	Y505H	D614G	H655Y	N679K	P681H	N764K	D796Y	Q954H	N969K			
	SARS-CoV-2_human_BHR_22020089582_S132_L001_2022	GenBank: OM843316.1	T19I	L24-	P25-	P26-	A27S		V213G	G339D	S371F	S373P	S375F	T376A	D405N	R408S	K417N	N440K	S477N	T478K	E484A	Q493R	Q498R	N501Y	Y505H	D614G	H655Y	N679K	P681H	N764K	D796Y	Q954H	N969K			
	SARS-CoV-2_human_BHR_22020090467_S157_L001_2022	GenBank: OM843340.1	T19I	L24-	P25-	P26-	A27S		V213G	G339D	S371F	S373P	S375F	T376A	D405N	R408S	K417N	N440K	S477N	T478K	E484A	Q493R	Q498R	N501Y	Y505H	D614G	H655Y	N679K	P681H	N764K	D796Y	Q954H	N969K			
	SARS-CoV-2_human_USA_NC-CDC-LC0562514_2022	GenBank: ON049267.1	T19I	L24-	P25-	P26-	A27S	G142D		G339D	S371F	S373P	S375F	T376A	D405N	R408S	K417N	N440K	S477N	T478K	E484A	Q493R	Q498R	N501Y	Y505H	D614G	H655Y	N679K	P681H	N764K	D796Y	Q954H	N969K		c25000u	
	SARS-CoV-2_human_USA_FL-CDC-LC0593238_2022	GenBank: ON450720.1	T19I	L24-	P25-	P26-	A27S	G142D		G339D	S371F	S373P	S375F	T376A	D405N	R408S	K417N	N440K	S477N	T478K	E484A	Q493R	Q498R	N501Y	Y505H	D614G	H655Y	N679K	P681H	N764K	D796Y	Q954H	N969K	c22792u	c25000u	c21859u
	SARS-CoV-2_human_USA_MA-CDC-ASC210721152_2022	GenBank: ON250163.1	T19I	L24-	P25-	P26-	A27S	G142D	V213G		S371F	S373P	S375F	T376A	D405N	R408S	K417N	N440K	S477N	T478K	E484A	Q493R	Q498R	N501Y	Y505H	D614G	H655Y	N679K	P681H	N764K	D796Y	Q954H	N969K	c22792u	c25000u	c22945u
	SARS-CoV-2_human_USA_OH-UHTL-2178_2022	GenBank: ON256603.1	T19I	L24-	P25-	P26-	A27S	G142D	V213G		S371F	S373P	S375F	T376A	D405N	R408S	K417N	N440K	S477N	T478K	E484A	Q493R	Q498R	N501Y	Y505H	D614G	H655Y	N679K	P681H	N764K	D796Y	Q954H	N969K		c25000u	
	SARS-CoV-2_human_USA_VSP12938_2022	GenBank: ON480422.1	T19I	L24-	P25-	P26-	A27S	G142D	V213G		S371F	S373P	S375F	T376A	D405N	R408S	K417N	N440K	S477N	T478K	E484A	Q493R	Q498R	N501Y	Y505H	D614G	H655Y	N679K	P681H	N764K	D796Y	Q954H	N969K	c22792u	c25000u	
	SARS-CoV-2_human_USA_NY-CDC-ASC210862593_2022	GenBank: OM888844.1	T19I	L24-	P25-	P26-	A27S	G142D	V213G	G339D		S373P	S375F	T376A	D405N	R408S	K417N	N440K	S477N	T478K	E484A	Q493R	Q498R	N501Y	Y505H	D614G	H655Y	N679K	P681H	N764K	D796Y	Q954H	N969K		c25000u	
	SARS-CoV-2_human_USA_NY-CDC-ASC210822042_2022	GenBank: OM890089.1	T19I	L24-	P25-	P26-	A27S	G142D	V213G	G339D		S373P	S375F	T376A	D405N	R408S	K417N	N440K	S477N	T478K	E484A	Q493R	Q498R	N501Y	Y505H	D614G	H655Y	N679K	P681H	N764K	D796Y	Q954H	N969K		c25000u	c23701u
	SARS-CoV-2_human_USA_OH-UHTL-2087_2022	GenBank: ON009425.2	T19I	L24-	P25-	P26-	A27S	G142D	V213G	G339D		S373P	S375F	T376A	D405N	R408S	K417N	N440K	S477N	T478K	E484A	Q493R	Q498R	N501Y	Y505H	D614G	H655Y	N679K	P681H	N764K	D796Y	Q954H	N969K		c25000u	
	SARS-CoV-2_human_USA_UT-UPHL-220318196385_2022	GenBank: ON082904.1	T19I	L24-	P25-	P26-	A27S	G142D	V213G	G339D		S373P	S375F	T376A	D405N	R408S	K417N	N440K	S477N	T478K	E484A	Q493R	Q498R	N501Y	Y505H	D614G	H655Y	N679K	P681H	N764K	D796Y	Q954H	N969K	c22792u	c25000u	
	SARS-CoV-2_human_USA_MA-CDC-ASC210821187_2022	GenBank: OM901275.1	T19I	L24-	P25-	P26-	A27S	G142D	V213G	G339D		S373P	S375F	T376A	D405N	R408S	K417N	N440K	S477N	T478K	E484A	Q493R	Q498R	N501Y	Y505H	D614G	H655Y	N679K	P681H	N764K	D796Y	Q954H	N969K		c25000u	
	SARS-CoV-2_human_USA_OH-UHTL-1997_2022	GenBank: OM877094.2	T19I	L24-	P25-	P26-	A27S	G142D	V213G	G339D	S371F		S375F	T376A	D405N	R408S	K417N	N440K	S477N	T478K	E484A	Q493R	Q498R	N501Y	Y505H	D614G	H655Y	N679K	P681H	N764K	D796Y	Q954H	N969K		c25000u	
	SARS-CoV-2_human_USA_OH-UHTL-1998_2022	GenBank: OM877095.2	T19I	L24-	P25-	P26-	A27S	G142D	V213G	G339D	S371F		S375F	T376A	D405N	R408S	K417N	N440K	S477N	T478K	E484A	Q493R	Q498R	N501Y	Y505H	D614G	H655Y	N679K	P681H	N764K	D796Y	Q954H	N969K		c25000u	
	SARS-CoV-2_human_USA_OH-UHTL-1999_2022	GenBank: OM877096.2	T19I	L24-	P25-	P26-	A27S	G142D	V213G	G339D	S371F		S375F	T376A	D405N	R408S	K417N	N440K	S477N	T478K	E484A	Q493R	Q498R	N501Y	Y505H	D614G	H655Y	N679K	P681H	N764K	D796Y	Q954H	N969K		c25000u	
	SARS-CoV-2_human_USA_OH-UHTL-2000_2022	GenBank: OM877097.2	T19I	L24-	P25-	P26-	A27S	G142D	V213G	G339D	S371F		S375F	T376A	D405N	R408S	K417N	N440K	S477N	T478K	E484A	Q493R	Q498R	N501Y	Y505H	D614G	H655Y	N679K	P681H	N764K	D796Y	Q954H	N969K		c25000u	
	SARS-CoV-2_human_USA_CO-CDC-MMB15007786_2022	GenBank: ON378542.1	T19I	L24-	P25-	P26-	A27S	G142D	V213G	G339D	S371F	S373P		T376A	D405N	R408S	K417N	N440K	S477N	T478K	E484A	Q493R	Q498R	N501Y	Y505H	D614G	H655Y	N679K	P681H	N764K	D796Y	Q954H	N969K		c25000u	
	SARS-CoV-2_human_USA_CO-CDC-MMB15041240_2022	GenBank: ON389858.1	T19I	L24-	P25-	P26-	A27S	G142D	V213G	G339D	S371F	S373P		T376A	D405N	R408S	K417N	N440K	S477N	T478K	E484A	Q493R	Q498R	N501Y	Y505H	D614G	H655Y	N679K	P681H	N764K	D796Y	Q954H	N969K		c25000u	
	SARS-CoV-2_human_USA_CO-CDC-MMB15051587_2022	GenBank: ON389889.1	T19I	L24-	P25-	P26-	A27S	G142D	V213G	G339D	S371F	S373P		T376A	D405N	R408S	K417N	N440K	S477N	T478K	E484A	Q493R	Q498R	N501Y	Y505H	D614G	H655Y	N679K	P681H	N764K	D796Y	Q954H	N969K		c25000u	c22987u
	SARS-CoV-2_human_USA_CO-CDC-MMB15083993_2022	GenBank: ON390359.1	T19I	L24-	P25-	P26-	A27S	G142D	V213G	G339D	S371F	S373P		T376A	D405N	R408S	K417N	N440K	S477N	T478K	E484A	Q493R	Q498R	N501Y	Y505H	D614G	H655Y	N679K	P681H	N764K	D796Y	Q954H	N969K		c25000u	
	SARS-CoV-2_human_USA_CO-CDC-MMB15083344_2022	GenBank: ON390365.1	T19I	L24-	P25-	P26-	A27S	G142D	V213G	G339D	S371F	S373P		T376A	D405N	R408S	K417N	N440K	S477N	T478K	E484A	Q493R	Q498R	N501Y	Y505H	D614G	H655Y	N679K	P681H	N764K	D796Y	Q954H	N969K		c25000u	
	SARS-CoV-2_human_USA_MN-CDC-IBX999279293948_2022	GenBank: OM936703.1	T19I	L24-	P25-	P26-	A27S	G142D	V213G	G339D	S371F	S373P	S375F		D405N	R408S	K417N	N440K	S477N	T478K	E484A	Q493R	Q498R	N501Y	Y505H	D614G	H655Y	N679K	P681H	N764K	D796Y	Q954H	N969K	c22792u	c25000u	a24433g
	SARS-CoV-2_human_USA_2081650_2022	GenBank: ON352711.1	T19I	L24-	P25-	P26-	A27S	G142D	V213G	G339D	S371F	S373P	S375F		D405N	R408S	K417N	N440K	S477N	T478K	E484A	Q493R	Q498R	N501Y	Y505H	D614G	H655Y	N679K	P681H	N764K	D796Y	Q954H	N969K		c25000u	
	SARS-CoV-2_human_USA_CO-CDC-MMB14969199_2022	GenBank: ON378000.1	T19I	L24-	P25-	P26-	A27S	G142D	V213G	G339D	S371F	S373P	S375F		D405N	R408S	K417N	N440K	S477N	T478K	E484A	Q493R	Q498R	N501Y	Y505H	D614G	H655Y	N679K	P681H	N764K	D796Y	Q954H	N969K		c25000u	
	SARS-CoV-2_human_USA_NY-CDC-QDX35135953_2022	GenBank: ON177702.1	T19I	L24-	P25-	P26-	A27S	G142D	V213G	G339D	S371F	S373P	S375F	T376A		R408S	K417N	N440K	S477N	T478K	E484A	Q493R	Q498R	N501Y	Y505H	D614G	H655Y	N679K	P681H	N764K	D796Y	Q954H	N969K		c25000u	
	SARS-CoV-2_human_USA_UT-UPHL-220403908426_2022	GenBank: ON205494.1	T19I	L24-	P25-	P26-	A27S	G142D	V213G	G339D	S371F	S373P	S375F	T376A		R408S	K417N	N440K	S477N	T478K	E484A	Q493R	Q498R	N501Y	Y505H	D614G	H655Y	N679K	P681H	N764K	D796Y	Q954H	N969K	c22792u	c25000u	a24433g
	SARS-CoV-2_human_USA_CO-CDC-MMB15023382_2022	GenBank: ON378633.1	T19I	L24-	P25-	P26-	A27S	G142D	V213G	G339D	S371F	S373P	S375F	T376A		R408S	K417N	N440K	S477N	T478K	E484A	Q493R	Q498R	N501Y	Y505H	D614G	H655Y	N679K	P681H	N764K	D796Y	Q954H	N969K		c25000u	
	SARS-CoV-2_human_USA_UT-UPHL-220519708663_2022	GenBank: ON617689.1	T19I	L24-	P25-	P26-	A27S	G142D	V213G	G339D	S371F	S373P	S375F	T376A		R408S	K417N	N440K	S477N	T478K	E484A	Q493R	Q498R	N501Y	Y505H	D614G	H655Y	N679K	P681H	N764K	D796Y	Q954H	N969K	c22792u	c25000u	
	SARS-CoV-2_human_USA_NY-PV58389_2022	GenBank: ON619375.1	T19I	L24-	P25-	P26-	A27S	G142D	V213G	G339D	S371F	S373P	S375F	T376A		R408S	K417N	N440K	S477N	T478K	E484A	Q493R	Q498R	N501Y	Y505H	D614G	H655Y	N679K	P681H	N764K	D796Y	Q954H	N969K	c22792u	c25000u	
	SARS-CoV-2_human_USA_GA-GPHL-734_2022	GenBank: OM567618.1	T19I	L24-	P25-	P26-	A27S	G142D	V213G	G339D	S371F	S373P	S375F	T376A	D405N		K417N	N440K	S477N	T478K	E484A	Q493R	Q498R	N501Y	Y505H	D614G	H655Y	N679K	P681H	N764K	D796Y	Q954H	N969K		c25000u	
	SARS-CoV-2_human_USA_MN-CDC-IBX322657542052_2022	GenBank: OM659585.1	T19I	L24-	P25-	P26-	A27S	G142D	V213G	G339D	S371F	S373P	S375F	T376A	D405N		K417N	N440K	S477N	T478K	E484A	Q493R	Q498R	N501Y	Y505H	D614G	H655Y	N679K	P681H	N764K	D796Y	Q954H	N969K		c25000u	
	SARS-CoV-2_human_USA_MA-CDC-ASC210651361_2022	GenBank: OM770913.1	T19I	L24-	P25-	P26-	A27S	G142D	V213G	G339D	S371F	S373P	S375F	T376A	D405N		K417N	N440K	S477N	T478K	E484A	Q493R	Q498R	N501Y	Y505H	D614G	H655Y	N679K	P681H	N764K	D796Y	Q954H	N969K		c25000u	
	SARS-CoV-2_human_USA_MN-CDC-IBX352441390588_2022	GenBank: OM781641.1	T19I	L24-	P25-	P26-	A27S	G142D	V213G	G339D	S371F	S373P	S375F	T376A	D405N		K417N	N440K	S477N	T478K	E484A	Q493R	Q498R	N501Y	Y505H	D614G	H655Y	N679K	P681H	N764K	D796Y	Q954H	N969K		c25000u	
	SARS-CoV-2_human_USA_MN-CDC-IBX076829438540_2022	GenBank: OM805865.1	T19I	L24-	P25-	P26-	A27S	G142D	V213G	G339D	S371F	S373P	S375F	T376A	D405N		K417N	N440K	S477N	T478K	E484A	Q493R	Q498R	N501Y	Y505H	D614G	H655Y	N679K	P681H	N764K	D796Y	Q954H	N969K		c25000u	
	SARS-CoV-2_human_BGD_Laila_918_2022	GenBank: OM533441.1	T19I	L24-	P25-	P26-	A27S	G142D	V213G	G339D	S371F	S373P	S375F	T376A	D405N	R408S		N440K	S477N	T478K	E484A	Q493R	Q498R	N501Y	Y505H	D614G	H655Y	N679K	P681H	N764K	D796Y	Q954H	N969K		c25000u	
	SARS-CoV-2_human_BGD_Laila_923_2022	GenBank: OM533458.1	T19I	L24-	P25-	P26-	A27S	G142D	V213G	G339D	S371F	S373P	S375F	T376A	D405N	R408S		N440K	S477N	T478K	E484A	Q493R	Q498R	N501Y	Y505H	D614G	H655Y	N679K	P681H	N764K	D796Y	Q954H	N969K		c25000u	
	SARS-CoV-2_human_BGD_Laila_872_2022	GenBank: OM570235.1	T19I	L24-	P25-	P26-	A27S	G142D	V213G	G339D	S371F	S373P	S375F	T376A	D405N	R408S		N440K	S477N	T478K	E484A	Q493R	Q498R	N501Y	Y505H	D614G	H655Y	N679K	P681H	N764K	D796Y	Q954H	N969K		c25000u	
	SARS-CoV-2_human_BGD_Laila_887_2022	GenBank: OM570249.1	T19I	L24-	P25-	P26-	A27S	G142D	V213G	G339D	S371F	S373P	S375F	T376A	D405N	R408S		N440K	S477N	T478K	E484A	Q493R	Q498R	N501Y	Y505H	D614G	H655Y	N679K	P681H	N764K	D796Y	Q954H	N969K		c25000u	
	SARS-CoV-2_human_BGD_Laila_879_2022	GenBank: OM570252.1	T19I	L24-	P25-	P26-	A27S	G142D	V213G	G339D	S371F	S373P	S375F	T376A	D405N	R408S		N440K	S477N	T478K	E484A	Q493R	Q498R	N501Y	Y505H	D614G	H655Y	N679K	P681H	N764K	D796Y	Q954H	N969K		c25000u	
	SARS-CoV-2_human_BHR_22120013600_S117_L001_2022	GenBank: OM283320.1	T19I	L24-	P25-	P26-	A27S	G142D	V213G	G339D	S371F	S373P	S375F	T376A	D405N	R408S	K417N		S477N	T478K	E484A	Q493R	Q498R	N501Y	Y505H	D614G	H655Y	N679K	P681H	N764K	D796Y	Q954H	N969K		c25000u	
	SARS-CoV-2_human_BHR_22120021978_S127_L001_2022	GenBank: OM283343.1	T19I	L24-	P25-	P26-	A27S	G142D	V213G	G339D	S371F	S373P	S375F	T376A	D405N	R408S	K417N		S477N	T478K	E484A	Q493R	Q498R	N501Y	Y505H	D614G	H655Y	N679K	P681H	N764K	D796Y	Q954H	N969K		c25000u	
	SARS-CoV-2_human_BHR_22120022463_S77_L001_2022	GenBank: OM283361.1	T19I	L24-	P25-	P26-	A27S	G142D	V213G	G339D	S371F	S373P	S375F	T376A	D405N	R408S	K417N		S477N	T478K	E484A	Q493R	Q498R	N501Y	Y505H	D614G	H655Y	N679K	P681H	N764K	D796Y	Q954H	N969K		c25000u	
	SARS-CoV-2_human_BHR_22120022464_S78_L001_2022	GenBank: OM283362.1	T19I	L24-	P25-	P26-	A27S	G142D	V213G	G339D	S371F	S373P	S375F	T376A	D405N	R408S	K417N		S477N	T478K	E484A	Q493R	Q498R	N501Y	Y505H	D614G	H655Y	N679K	P681H	N764K	D796Y	Q954H	N969K		c25000u	
	SARS-CoV-2_human_BHR_22120022949_S81_L001_2022	GenBank: OM283368.1	T19I	L24-	P25-	P26-	A27S	G142D	V213G	G339D	S371F	S373P	S375F	T376A	D405N	R408S	K417N		S477N	T478K	E484A	Q493R	Q498R	N501Y	Y505H	D614G	H655Y	N679K	P681H	N764K	D796Y	Q954H	N969K		c25000u	
	SARS-CoV-2_human_USA_CA-CDPH-8000000127_2022	GenBank: ON618014.1	T19I	L24-	P25-	P26-	A27S	G142D	V213G	G339D	S371F	S373P	S375F	T376A	D405N	R408S	K417N	N440K		T478K	E484A	Q493R	Q498R	N501Y	Y505H	D614G	H655Y	N679K	P681H	N764K	D796Y	Q954H	N969K		c25000u	
	SARS-CoV-2_human_USA_CA-CDPH-8000000133_2022	GenBank: ON618018.1	T19I	L24-	P25-	P26-	A27S	G142D	V213G	G339D	S371F	S373P	S375F	T376A	D405N	R408S	K417N	N440K		T478K	E484A	Q493R	Q498R	N501Y	Y505H	D614G	H655Y	N679K	P681H	N764K	D796Y	Q954H	N969K		c25000u	c23347u
	SARS-CoV-2_human_USA_CA-CDPH-8000000134_2022	GenBank: ON618019.1	T19I	L24-	P25-	P26-	A27S	G142D	V213G	G339D	S371F	S373P	S375F	T376A	D405N	R408S	K417N	N440K		T478K	E484A	Q493R	Q498R	N501Y	Y505H	D614G	H655Y	N679K	P681H	N764K	D796Y	Q954H	N969K		c25000u	
	SARS-CoV-2_human_USA_CA-CDPH-8000000146_2022	GenBank: ON618027.1	T19I	L24-	P25-	P26-	A27S	G142D	V213G	G339D	S371F	S373P	S375F	T376A	D405N	R408S	K417N	N440K		T478K	E484A	Q493R	Q498R	N501Y	Y505H	D614G	H655Y	N679K	P681H	N764K	D796Y	Q954H	N969K		c25000u	
	SARS-CoV-2_human_USA_CA-CDPH-2000066893_2022	GenBank: ON618363.1	T19I	L24-	P25-	P26-	A27S	G142D	V213G	G339D	S371F	S373P	S375F	T376A	D405N	R408S	K417N	N440K		T478K	E484A	Q493R	Q498R	N501Y	Y505H	D614G	H655Y	N679K	P681H	N764K	D796Y	Q954H	N969K		c25000u	
	SARS-CoV-2_human_USA_IL-CDC-QDX35624690_2022	GenBank: ON311615.1	T19I	L24-	P25-	P26-	A27S	G142D	V213G	G339D	S371F	S373P	S375F	T376A	D405N	R408S	K417N	N440K	S477N	T478K		Q493R	Q498R	N501Y	Y505H	D614G	H655Y	N679K	P681H	N764K	D796Y	Q954H	N969K		c25000u	
	SARS-CoV-2_human_USA_CA-SLOPH-C1219_2022	GenBank: ON383919.1	T19I	L24-	P25-	P26-	A27S	G142D	V213G	G339D	S371F	S373P	S375F	T376A	D405N	R408S	K417N	N440K	S477N	T478K		Q493R	Q498R	N501Y	Y505H	D614G	H655Y	N679K	P681H	N764K	D796Y	Q954H	N969K		c25000u	
	SARS-CoV-2_human_THA_CONI-3664_2022	GenBank: OP579158.1	T19I	L24-	P25-	P26-	A27S	G142D	V213G	G339D	S371F	S373P	S375F	T376A	D405N	R408S	K417N	N440K	S477N	T478K		Q493R	Q498R	N501Y	Y505H	D614G	H655Y	N679K	P681H	N764K	D796Y	Q954H	N969K		c25000u	u24640c
	SARS-CoV-2_human_USA_PA-CDC-QDX38634742_2022	GenBank: OP054411.1	T19I	L24-	P25-	P26-	A27S	G142D	V213G	G339D	S371F	S373P	S375F	T376A	D405N	R408S	K417N	N440K	S477N	T478K		Q493R	Q498R	N501Y	Y505H	D614G	H655Y	N679K	P681H	N764K	D796Y	Q954H	N969K		c25000u	
	SARS-CoV-2_human_USA_TX-CDC-QDX36807347_2022	GenBank: ON633107.1	T19I	L24-	P25-	P26-	A27S	G142D	V213G	G339D	S371F	S373P	S375F	T376A	D405N	R408S	K417N	N440K	S477N	T478K		Q493R	Q498R	N501Y	Y505H	D614G	H655Y	N679K	P681H	N764K	D796Y	Q954H	N969K	c22792u	c25000u	a24619g
	SARS-CoV-2_human_USA_OR-CDC-LC0590554_2022	GenBank: ON414693.1	T19I	L24-	P25-	P26-	A27S	G142D	V213G	G339D	S371F	S373P	S375F	T376A	D405N	R408S	K417N	N440K	S477N	T478K	E484A		Q498R	N501Y	Y505H	D614G	H655Y	N679K	P681H	N764K	D796Y	Q954H	N969K		c25000u	c24865u
	SARS-CoV-2_human_USA_FL-CDC-STM-9ETNSYQ68_2022	GenBank: ON422887.1	T19I	L24-	P25-	P26-	A27S	G142D	V213G	G339D	S371F	S373P	S375F	T376A	D405N	R408S	K417N	N440K	S477N	T478K	E484A		Q498R	N501Y	Y505H	D614G	H655Y	N679K	P681H	N764K	D796Y	Q954H	N969K		c25000u	
	SARS-CoV-2_human_USA_E8DAF5E01C0_2022	GenBank: OP364296.1	T19I	L24-	P25-	P26-	A27S	G142D	V213G	G339D	S371F	S373P	S375F	T376A	D405N	R408S	K417N	N440K	S477N	T478K	E484A		Q498R	N501Y	Y505H	D614G	H655Y	N679K	P681H	N764K	D796Y	Q954H	N969K		c25000u	
	SARS-CoV-2_human_USA_TMCL-022A Nasal Swab_2022	GenBank: OP629673.1	T19I	L24-	P25-	P26-	A27S	G142D	V213G	G339D	S371F	S373P	S375F	T376A	D405N	R408S	K417N	N440K	S477N	T478K	E484A		Q498R	N501Y	Y505H	D614G	H655Y	N679K	P681H	N764K	D796Y	Q954H	N969K		c25000u	
	SARS-CoV-2_human_USA_CA-CDC-QDX35734313_2022	GenBank: ON363097.1	T19I	L24-	P25-	P26-	A27S	G142D	V213G	G339D	S371F	S373P	S375F	T376A	D405N	R408S	K417N	N440K	S477N	T478K	E484A	Q493R		N501Y	Y505H	D614G	H655Y	N679K	P681H	N764K	D796Y	Q954H	N969K	c22792u	c25000u	
	SARS-CoV-2_human_NZL_22CH3603_2022	GenBank: OP633561.1	T19I	L24-	P25-	P26-	A27S	G142D	V213G	G339D	S371F	S373P	S375F	T376A	D405N	R408S	K417N	N440K	S477N	T478K	E484A	Q493R		N501Y	Y505H	D614G	H655Y	N679K	P681H	N764K	D796Y	Q954H	N969K		c25000u	
	SARS-CoV-2_human_USA_CA-CDC-QDX35974755_2022	GenBank: ON458445.1	T19I	L24-	P25-	P26-	A27S	G142D	V213G	G339D	S371F	S373P	S375F	T376A	D405N	R408S	K417N	N440K	S477N	T478K	E484A	Q493R		N501Y	Y505H	D614G	H655Y	N679K	P681H	N764K	D796Y	Q954H	N969K		c25000u	
	SARS-CoV-2_human_USA_NJ-CDC-LC0630974_2022	GenBank: ON592247.1	T19I	L24-	P25-	P26-	A27S	G142D	V213G	G339D	S371F	S373P	S375F	T376A	D405N	R408S	K417N	N440K	S477N	T478K	E484A	Q493R		N501Y	Y505H	D614G	H655Y	N679K	P681H	N764K	D796Y	Q954H	N969K		c25000u	
	SARS-CoV-2_human_USA_NY-CDC-QDX36604947_2022	GenBank: ON549687.1	T19I	L24-	P25-	P26-	A27S	G142D	V213G	G339D	S371F	S373P	S375F	T376A	D405N	R408S	K417N	N440K	S477N	T478K	E484A	Q493R		N501Y	Y505H	D614G	H655Y	N679K	P681H	N764K	D796Y	Q954H	N969K		c25000u	
	SARS-CoV-2_human_USA_MA-Broad-CRSP_RONTL6TVQ6F4W7SU_2022	GenBank: ON067040.1	T19I	L24-	P25-	P26-	A27S	G142D	V213G	G339D	S371F	S373P	S375F	T376A	D405N	R408S	K417N	N440K	S477N	T478K	E484A	Q493R	Q498R		Y505H	D614G	H655Y	N679K	P681H	N764K	D796Y	Q954H	N969K		c25000u	
	SARS-CoV-2_human_USA_NY-Broad-CRSP_W5RRSQYSNEU2CTCC_2022	GenBank: ON199452.1	T19I	L24-	P25-	P26-	A27S	G142D	V213G	G339D	S371F	S373P	S375F	T376A	D405N	R408S	K417N	N440K	S477N	T478K	E484A	Q493R	Q498R		Y505H	D614G	H655Y	N679K	P681H	N764K	D796Y	Q954H	N969K		c25000u	
	SARS-CoV-2_human_USA_MA-Broad-CRSP_HI2VSRB3HJJCYJLN_2022	GenBank: ON200331.1	T19I	L24-	P25-	P26-	A27S	G142D	V213G	G339D	S371F	S373P	S375F	T376A	D405N	R408S	K417N	N440K	S477N	T478K	E484A	Q493R	Q498R		Y505H	D614G	H655Y	N679K	P681H	N764K	D796Y	Q954H	N969K	c22792u	c25000u	
	SARS-CoV-2_human_USA_MA-Broad-CRSP_OTZ2XP3IC3O2MGXT_2022	GenBank: ON200438.1	T19I	L24-	P25-	P26-	A27S	G142D	V213G	G339D	S371F	S373P	S375F	T376A	D405N	R408S	K417N	N440K	S477N	T478K	E484A	Q493R	Q498R		Y505H	D614G	H655Y	N679K	P681H	N764K	D796Y	Q954H	N969K		c25000u	
	SARS-CoV-2_human_USA_VT-Broad-CRSP_BASF6SBPTLBI5WS5_2022	GenBank: ON321116.1	T19I	L24-	P25-	P26-	A27S	G142D	V213G	G339D	S371F	S373P	S375F	T376A	D405N	R408S	K417N	N440K	S477N	T478K	E484A	Q493R	Q498R		Y505H	D614G	H655Y	N679K	P681H	N764K	D796Y	Q954H	N969K		c25000u	
	SARS-CoV-2_human_USA_CA-CDC-ASC210859265_2022	GenBank: OM861064.1	T19I	L24-	P25-	P26-	A27S	G142D	V213G	G339D	S371F	S373P	S375F	T376A	D405N	R408S	K417N	N440K	S477N	T478K	E484A	Q493R	Q498R	N501Y		D614G	H655Y	N679K	P681H	N764K	D796Y	Q954H	N969K		c25000u	
	SARS-CoV-2_human_USA_FL-CDC-ASC210731143_2022	GenBank: OM969592.1	T19I	L24-	P25-	P26-	A27S	G142D	V213G	G339D	S371F	S373P	S375F	T376A	D405N	R408S	K417N	N440K	S477N	T478K	E484A	Q493R	Q498R	N501Y		D614G	H655Y	N679K	P681H	N764K	D796Y	Q954H	N969K		c25000u	
	SARS-CoV-2_human_USA_CA-CDC-ASC210757440_2022	GenBank: ON019120.1	T19I	L24-	P25-	P26-	A27S	G142D	V213G	G339D	S371F	S373P	S375F	T376A	D405N	R408S	K417N	N440K	S477N	T478K	E484A	Q493R	Q498R	N501Y		D614G	H655Y	N679K	P681H	N764K	D796Y	Q954H	N969K		c25000u	
	SARS-CoV-2_human_USA_NY-PBRI-22M007_2022	GenBank: ON221860.1	T19I	L24-	P25-	P26-	A27S	G142D	V213G	G339D	S371F	S373P	S375F	T376A	D405N	R408S	K417N	N440K	S477N	T478K	E484A	Q493R	Q498R	N501Y		D614G	H655Y	N679K	P681H	N764K	D796Y	Q954H	N969K		c25000u	
	SARS-CoV-2_human_USA_NY-PBRI-22M008_2022	GenBank: ON221861.1	T19I	L24-	P25-	P26-	A27S	G142D	V213G	G339D	S371F	S373P	S375F	T376A	D405N	R408S	K417N	N440K	S477N	T478K	E484A	Q493R	Q498R	N501Y		D614G	H655Y	N679K	P681H	N764K	D796Y	Q954H	N969K		c25000u	
	SARS-CoV-2_human_USA_TX-CDC-ASC210858963_2022	GenBank: OM861619.1	T19I	L24-	P25-	P26-	A27S	G142D	V213G	G339D	S371F	S373P	S375F	T376A	D405N	R408S	K417N	N440K	S477N	T478K	E484A	Q493R	Q498R	N501Y	Y505H		H655Y	N679K	P681H	N764K	D796Y	Q954H	N969K		c25000u	
	SARS-CoV-2_human_USA_PA-CDC-LC0564604_2022	GenBank: ON091288.1	T19I	L24-	P25-	P26-	A27S	G142D	V213G	G339D	S371F	S373P	S375F	T376A	D405N	R408S	K417N	N440K	S477N	T478K	E484A	Q493R	Q498R	N501Y	Y505H		H655Y	N679K	P681H	N764K	D796Y	Q954H	N969K		c25000u	
	SARS-CoV-2_human_USA_CT-CDC-LC0566727_2022	GenBank: ON151370.1	T19I	L24-	P25-	P26-	A27S	G142D	V213G	G339D	S371F	S373P	S375F	T376A	D405N	R408S	K417N	N440K	S477N	T478K	E484A	Q493R	Q498R	N501Y	Y505H		H655Y	N679K	P681H	N764K	D796Y	Q954H	N969K		c25000u	
	SARS-CoV-2_human_USA_NJ-CDC-LC0569045_2022	GenBank: ON233850.1	T19I	L24-	P25-	P26-	A27S	G142D	V213G	G339D	S371F	S373P	S375F	T376A	D405N	R408S	K417N	N440K	S477N	T478K	E484A	Q493R	Q498R	N501Y	Y505H		H655Y	N679K	P681H	N764K	D796Y	Q954H	N969K		c25000u	
	SARS-CoV-2_human_USA_CT-CDC-ASC210849642_2022	GenBank: ON236456.1	T19I	L24-	P25-	P26-	A27S	G142D	V213G	G339D	S371F	S373P	S375F	T376A	D405N	R408S	K417N	N440K	S477N	T478K	E484A	Q493R	Q498R	N501Y	Y505H		H655Y	N679K	P681H	N764K	D796Y	Q954H	N969K		c25000u	
	SARS-CoV-2_human_USA_CT-CDC-LC0575807_2022	GenBank: ON296711.1	T19I	L24-	P25-	P26-	A27S	G142D	V213G	G339D	S371F	S373P	S375F	T376A	D405N	R408S	K417N	N440K	S477N	T478K	E484A	Q493R	Q498R	N501Y	Y505H	D614G		N679K	P681H	N764K	D796Y	Q954H	N969K	c22792u	c25000u	
	SARS-CoV-2_human_USA_NY-CDC-LC0610786_2022	GenBank: ON535443.1	T19I	L24-	P25-	P26-	A27S	G142D	V213G	G339D	S371F	S373P	S375F	T376A	D405N	R408S	K417N	N440K	S477N	T478K	E484A	Q493R	Q498R	N501Y	Y505H	D614G		N679K	P681H	N764K	D796Y	Q954H	N969K	c22792u	c25000u	a23989g; u23047c
	SARS-CoV-2_human_USA_NY-CDC-LC0642966_2022	GenBank: ON624524.1	T19I	L24-	P25-	P26-	A27S	G142D	V213G	G339D	S371F	S373P	S375F	T376A	D405N	R408S	K417N	N440K	S477N	T478K	E484A	Q493R	Q498R	N501Y	Y505H	D614G		N679K	P681H	N764K	D796Y	Q954H	N969K		c25000u	
	SARS-CoV-2_human_USA_NJ-CDC-LC0583804_2022	GenBank: ON377450.1	T19I	L24-	P25-	P26-	A27S	G142D	V213G	G339D	S371F	S373P	S375F	T376A	D405N	R408S	K417N	N440K	S477N	T478K	E484A	Q493R	Q498R	N501Y	Y505H	D614G		N679K	P681H	N764K	D796Y	Q954H	N969K		c25000u	u24346c
	SARS-CoV-2_human_USA_DC-CDC-LC0587755_2022	GenBank: ON397268.1	T19I	L24-	P25-	P26-	A27S	G142D	V213G	G339D	S371F	S373P	S375F	T376A	D405N	R408S	K417N	N440K	S477N	T478K	E484A	Q493R	Q498R	N501Y	Y505H	D614G		N679K	P681H	N764K	D796Y	Q954H	N969K		c25000u	
	SARS-CoV-2_human_USA_NJ-PHEL-V22016186_2022	GenBank: ON239032.1	T19I	L24-	P25-	P26-	A27S	G142D	V213G	G339D	S371F	S373P	S375F	T376A	D405N	R408S	K417N	N440K	S477N	T478K	E484A	Q493R	Q498R	N501Y	Y505H	D614G	H655Y		P681H	N764K	D796Y	Q954H	N969K		c25000u	c21811u; c21952u
	SARS-CoV-2_human_USA_WA-CDC-LC0581940_2022	GenBank: ON373649.1	T19I	L24-	P25-	P26-	A27S	G142D	V213G	G339D	S371F	S373P	S375F	T376A	D405N	R408S	K417N	N440K	S477N	T478K	E484A	Q493R	Q498R	N501Y	Y505H	D614G	H655Y		P681H	N764K	D796Y	Q954H	N969K	c22792u	c25000u	
	SARS-CoV-2_human_USA_CA-CDC-STM-Q8JDYJ7WW_2022	GenBank: ON481637.1	T19I	L24-	P25-	P26-	A27S	G142D	V213G	G339D	S371F	S373P	S375F	T376A	D405N	R408S	K417N	N440K	S477N	T478K	E484A	Q493R	Q498R	N501Y	Y505H	D614G	H655Y		P681H	N764K	D796Y	Q954H	N969K		c25000u	
	SARS-CoV-2_human_USA_MD-CDC-LC0651160_2022	GenBank: ON701163.1	T19I	L24-	P25-	P26-	A27S	G142D	V213G	G339D	S371F	S373P	S375F	T376A	D405N	R408S	K417N	N440K	S477N	T478K	E484A	Q493R	Q498R	N501Y	Y505H	D614G	H655Y		P681H	N764K	D796Y	Q954H	N969K	c22792u	c25000u	a22753u
	SARS-CoV-2_human_USA_MI-CDC-ASC210729927_2022	GenBank: OM948079.1	T19I	L24-	P25-	P26-	A27S	G142D	V213G	G339D	S371F	S373P	S375F	T376A	D405N	R408S	K417N	N440K	S477N	T478K	E484A	Q493R	Q498R	N501Y	Y505H	D614G	H655Y		P681H	N764K	D796Y	Q954H	N969K		c25000u	
	SARS-CoV-2_human_USA_UT-UPHL-220417292921_2022	GenBank: ON312677.1	T19I	L24-	P25-	P26-	A27S	G142D	V213G	G339D	S371F	S373P	S375F	T376A	D405N	R408S	K417N	N440K	S477N	T478K	E484A	Q493R	Q498R	N501Y	Y505H	D614G	H655Y	N679K	P681H		D796Y	Q954H	N969K		c25000u	c23635u
	SARS-CoV-2_human_USA_NC-CDC-LC0577859_2022	GenBank: ON349263.1	T19I	L24-	P25-	P26-	A27S	G142D	V213G	G339D	S371F	S373P	S375F	T376A	D405N	R408S	K417N	N440K	S477N	T478K	E484A	Q493R	Q498R	N501Y	Y505H	D614G	H655Y	N679K	P681H		D796Y	Q954H	N969K		c25000u	
	SARS-CoV-2_human_USA_DC-CDC-LC0583490_2022	GenBank: ON377487.1	T19I	L24-	P25-	P26-	A27S	G142D	V213G	G339D	S371F	S373P	S375F	T376A	D405N	R408S	K417N	N440K	S477N	T478K	E484A	Q493R	Q498R	N501Y	Y505H	D614G	H655Y	N679K	P681H		D796Y	Q954H	N969K	c22792u	c25000u	
	SARS-CoV-2_human_USA_VA-CDC-LC0583763_2022	GenBank: ON377609.1	T19I	L24-	P25-	P26-	A27S	G142D	V213G	G339D	S371F	S373P	S375F	T376A	D405N	R408S	K417N	N440K	S477N	T478K	E484A	Q493R	Q498R	N501Y	Y505H	D614G	H655Y	N679K	P681H		D796Y	Q954H	N969K		c25000u	
	SARS-CoV-2_human_USA_VA-CDC-LC0558906_2022	GenBank: OM989887.1	T19I	L24-	P25-	P26-	A27S	G142D	V213G	G339D	S371F	S373P	S375F	T376A	D405N	R408S	K417N	N440K	S477N	T478K	E484A	Q493R	Q498R	N501Y	Y505H	D614G	H655Y	N679K	P681H		D796Y	Q954H	N969K		c25000u	
	SARS-CoV-2_human_BGD_Laila_900_2022	GenBank: OM638574.1	T19I	L24-	P25-	P26-	A27S	G142D	V213G	G339D	S371F	S373P	S375F	T376A	D405N	R408S	K417N	N440K	S477N	T478K	E484A	Q493R	Q498R	N501Y	Y505H	D614G	H655Y	N679K	P681H	N764K		Q954H	N969K		c25000u	
	SARS-CoV-2_human_USA_MA-CDC-ASC210751149_2022	GenBank: OM911616.1	T19I	L24-	P25-	P26-	A27S	G142D	V213G	G339D	S371F	S373P	S375F	T376A	D405N	R408S	K417N	N440K	S477N	T478K	E484A	Q493R	Q498R	N501Y	Y505H	D614G	H655Y	N679K	P681H	N764K		Q954H	N969K		c25000u	
	SARS-CoV-2_human_BHR_470028530_2022	GenBank: OM988767.1	T19I	L24-	P25-	P26-	A27S	G142D	V213G	G339D	S371F	S373P	S375F	T376A	D405N	R408S	K417N	N440K	S477N	T478K	E484A	Q493R	Q498R	N501Y	Y505H	D614G	H655Y	N679K	P681H	N764K		Q954H	N969K		c25000u	
	SARS-CoV-2_human_USA_KS-CDC-ASC210757836_2022	GenBank: ON019770.1	T19I	L24-	P25-	P26-	A27S	G142D	V213G	G339D	S371F	S373P	S375F	T376A	D405N	R408S	K417N	N440K	S477N	T478K	E484A	Q493R	Q498R	N501Y	Y505H	D614G	H655Y	N679K	P681H	N764K		Q954H	N969K		c25000u	c24023u
	SARS-CoV-2_human_BHR_500109885_2022	GenBank: OM988769.1	T19I	L24-	P25-	P26-	A27S	G142D	V213G	G339D	S371F	S373P	S375F	T376A	D405N	R408S	K417N	N440K	S477N	T478K	E484A	Q493R	Q498R	N501Y	Y505H	D614G	H655Y	N679K	P681H	N764K		Q954H	N969K		c25000u	c24382u
	SARS-CoV-2_human_USA_NC-CDC-LC0598357_2022	GenBank: ON468158.1	T19I	L24-	P25-	P26-	A27S	G142D	V213G	G339D	S371F	S373P	S375F	T376A	D405N	R408S	K417N	N440K	S477N	T478K	E484A	Q493R	Q498R	N501Y	Y505H	D614G	H655Y	N679K	P681H	N764K	D796Y		N969K		c25000u	
	SARS-CoV-2_human_USA_NC-CDC-LC0636034_2022	GenBank: ON608924.1	T19I	L24-	P25-	P26-	A27S	G142D	V213G	G339D	S371F	S373P	S375F	T376A	D405N	R408S	K417N	N440K	S477N	T478K	E484A	Q493R	Q498R	N501Y	Y505H	D614G	H655Y	N679K	P681H	N764K	D796Y		N969K	c22792u	c25000u	
	SARS-CoV-2_human_USA_OH-UHTL-2312_2022	GenBank: ON604965.1	T19I	L24-	P25-	P26-	A27S	G142D	V213G	G339D	S371F	S373P	S375F	T376A	D405N	R408S	K417N	N440K	S477N	T478K	E484A	Q493R	Q498R	N501Y	Y505H	D614G	H655Y	N679K	P681H	N764K	D796Y		N969K		c25000u	
	SARS-CoV-2_human_USA_CA-CDC-LC0617566_2022	GenBank: ON535763.1	T19I	L24-	P25-	P26-	A27S	G142D	V213G	G339D	S371F	S373P	S375F	T376A	D405N	R408S	K417N	N440K	S477N	T478K	E484A	Q493R	Q498R	N501Y	Y505H	D614G	H655Y	N679K	P681H	N764K	D796Y		N969K		c25000u	
	SARS-CoV-2_human_USA_CO-CDC-MMB14986462_2022	GenBank: ON378227.1	T19I	L24-	P25-	P26-	A27S	G142D	V213G	G339D	S371F	S373P	S375F	T376A	D405N	R408S	K417N	N440K	S477N	T478K	E484A	Q493R	Q498R	N501Y	Y505H	D614G	H655Y	N679K	P681H	N764K	D796Y	Q954H		c22792u	c25000u	c22572u
	SARS-CoV-2_human_USA_GA-CDC-MMB14986912_2022	GenBank: ON378238.1	T19I	L24-	P25-	P26-	A27S	G142D	V213G	G339D	S371F	S373P	S375F	T376A	D405N	R408S	K417N	N440K	S477N	T478K	E484A	Q493R	Q498R	N501Y	Y505H	D614G	H655Y	N679K	P681H	N764K	D796Y	Q954H		c22792u	c25000u	
	SARS-CoV-2_human_USA_VA-CDC-LC0673698_2022	GenBank: ON728470.1	T19I	L24-	P25-	P26-	A27S	G142D	V213G	G339D	S371F	S373P	S375F	T376A	D405N	R408S	K417N	N440K	S477N	T478K	E484A	Q493R	Q498R	N501Y	Y505H	D614G	H655Y	N679K	P681H	N764K	D796Y	Q954H		c22792u	c25000u	

Supplemental Figure 3

A

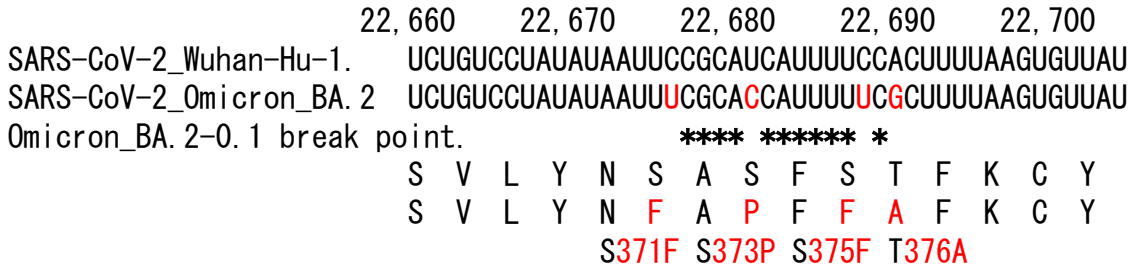

B